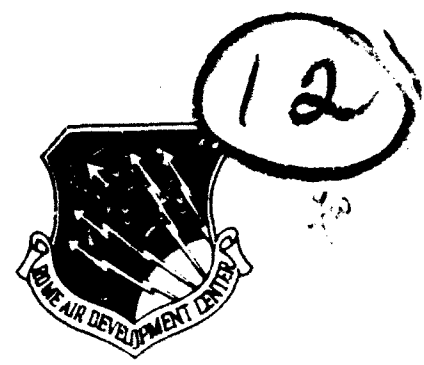RADC-TR-80-262
Final Technical Report
August 1980

LEVEL II

LARGE SIGNAL TWT COMPUTER THEORY

Hughes Aircraft Company

Dr. Tore Wessel-Berg

DTIC
S ELECTE
OCT 24 1980
F

AD A090748

ROME AIR DEVELOPMENT CENTER
Air Force Systems Command
Griffiss Air Force Base, New York 13441

DDC FILE_COPY

80 10 23 012

This report has been reviewed by the RADC Public 'ffairs Office (PA) and is releasable to the National Technical Information S. rvice (NTIS). At NTIS it will be releasable to the general public, including foreign nations.

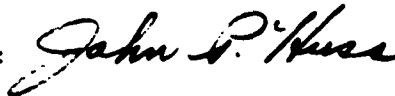RADC-TR-80-262 has been reviewed and is approved for publication.

APPROVED:

JOSEPH J. POLNIASZEK
Project Engineer

APPROVED:

FRANK J. REHM
Technical Director
Surveillance Division

FOR THE COMMANDER:

JOHN P. HUSS
Acting Chief, Plans Office

If your address has changed or if you wish to be removed from the RADC
mailing list, or if the addressee is no longer employed by your organization,
please notify RADC (OCTP) Griffiss AFB NY 13441. This will assist us in
maintaining a current mailing list.

Do not return this copy. Retain or destroy.

REPORT DOCUMENTATION PAGE		READ INSTRUCTIONS BEFORE COMPLETING FORM
1. REPORT NUMBER RADC-TR-80-262	2. GOVT ACCESSION NO.	3. RECIPIENT'S CATALOG NUMBER
4. TITLE (and Subtitle) LARGE SIGNAL TWT COMPUTER THEORY		5. TYPE OF REPORT & PERIOD COVERED Final Technical Report December 1978 - April 1980
		6. PERFORMING ORG. REPORT NUMBER W-08146
7. AUTHOR(s) Tore Wessel-Berg		8. CONTRACT OR GRANT NUMBER(s) F30602-79-C-0028
9. PERFORMING ORGANIZATION NAME AND ADDRESS Hughes Aircraft Company 3100 W. Lomita Blvd Torrance CA 90509		10. PROGRAM ELEMENT PROJECT, TASK AREA & WORK UNIT NUMBERS 62702F 45061243
11. CONTROLLING OFFICE NAME AND ADDRESS Rome Air Development Center (OCTP) Griffiss AFB NY 13441		12. REPORT DATE August 1980
		13. NUMBER OF PAGES 86
14. MONITORING AGENCY NAME & ADDRESS(if different from Controlling Office) Same		15. SECURITY CLASS. (of this report) UNCLASSIFIED
		15a. DECLASSIFICATION DOWNGRADING SCHEDULE N/A

16. DISTRIBUTION STATEMENT (of this Report)

Approved for public release; distribution unlimited

17. DISTRIBUTION STATEMENT (of the abstract entered in Block 20, if different from Report)

Same

18. SUPPLEMENTARY NOTES

RADC Project Engineer: Joseph J. Polniaszek (OCTP)

19. KEY WORDS (Continue on reverse side if necessary and identify by block number)

Large Signal TWT - Computer Theory
(Variable circuit parameters along the axis, backward wave
 instabilities)

20. ABSTRACT (Continue on reverse side if necessary and identify by block number)

Work reported here is a continuation of a previous effort described in
"Development of a Large Signal Computer Theory for TWT," based on polari-
zation variables reported on AFSC Contract F30607-77-C-0221.

The implementation of variable circuit parameters along the axis involves
the handling of velocity tapers, impedance tapers, and variable attenuator
sections, all in any prescribed fashion. ——   (over)

DD FORM 1473   EDITION OF 1 NOV 65 IS OBSOLETE

The second area is concerned with analysis of backward wave instabilities under the same conditions of variable parameters along the tube. In particular, the theory is applicable for segmented TWTs, i.e., tubes with several sections of otherwise constant circuit parameters. Such configurations are known to reduce backward wave instabilities, but the underlying theoretical background and the modeling have been inadequate. In particular, the symmetries and coupling relations of beam and circuit modes have not been sufficiently well understood. The present work is an effort to contribute to a better understanding of these effects and provide improved models and mathematical procedures for use in numerical analysis of backward wave instabilities.

One part of the investigation is the analysis of the properties of the beam modes involved in backward wave interactions. These have different symmetries from the usual circularly symmetric modes involved in forward interaction, and need special consideration.

The analysis of the stated problems involves a considerable mathematical apparatus, and all details cannot be contained in a relatively short final report. In particular, this applies to the analysis of the beam modes. On the other hand, a fairly complete account is presented of the backward wave instability problem.

The backward wave interaction analysis has been made with the assumption of confined-flow-focusing. It appears possible to extend the analysis to Brillouin-flow-focusing with uniform or periodic magnetic fields.

Accession For

NTIS GRA&I ☒
DTIC TAB ☐
Unannounced ☐
Justification

P

Distribution/

Availability Codes

Dist | Avail and/or
     | Special

A

PREFACE

This final technical report was authorized by Dr. T. Wessel-Berg and prepared by Electron Dynamics Division, Hughes Aircraft Company, Torrance, California, on Contract F30602-79-C-0028 for Rome Air Development Center, Griffiss Air Force Base, New York. It summarizes the results of a continuation effort on the "Development of a Large Signal Computer Theory for TWT," based on polarization variables that was reported on Contract F30602-77-C-0221. This continuation effort describes the implementation of variable circuit parameters along the tube axis, and provides a stability analysis of backward wave interaction, based on the assumption of confined-flow-focusing.

This effort has been initiated in December 1978 and was completed in March 1980. Joseph Polniaszek was RADC Project Engineer.

TABLE OF CONTENTS

TABLE OF CONTENTS (CONTINUED)

LIST OF ILLUSTRATIONS

EVALUATION

This report describes a novel approach to large signal modeling
of a helix type TWT. It embodies the benefits of increased accuracy
and decreased computation time for initial tube modeling and develop-
ment. This is accomplished through the use of a transformation
that reduces the nonlinear equations describing the system into a
set of linear differential equations that can be solved using classi-
cal techniques. The ultimate benefit of this program will be de-
creased development time and cost through a reduction in the com-
putation time and also the "cut and dry" experimental techniques
used presently.
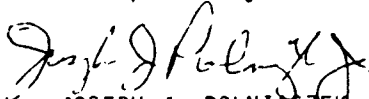
JOSEPH J. POLNIASZER
Project Engineer

1.0 INTRODUCTION

This report presents continuation efforts in the large signal computer theory described in report No. W-07587. It represents a further investigation of special effects and conditions of importance in TWT design. In particular, it treats two main areas: Implementation of variable circuit parameters along the tube, and backward wave instabilities.

The first of these main areas involves the handling of velocity tapers, impedance tapers, and variable attenuator sections, all in any prescribed fashion.

The second area is concerned with analysis of backward wave instabilities under the same conditions of variable parameters along the tube. In particular, the theory is applicable for segmented TWTs, i.e., tubes with several sections of otherwise constant circuit parameters. Such configurations are known to reduce backward wave instabilities, but the underlying theoretical background and the modeling have been inadequate. In particular, the symmetries and coupling relations of beam and circuit modes have not been sufficiently well understood. The present work is an effort to contribute to a better understanding of these effects and provide improved models and mathematical procedures for use in numerical analysis of backward wave instabilities.

One part of the investigation is the analysis of the properties of the beam modes involved in backward wave interactions. These have different symmetries from the usual circularly symmetric modes involved in forward interaction, and need special consideration.

The analysis of the stated problems involves a considerable mathematical apparatus, and all details can not be contained in a relatively short final report. In particular, this applies to the analysis of the beam modes. On the other hand, a fairly complete account is presented of the backward wave instability problem.

1

2.0 THE TREATMENT OF TAPERED CIRCUIT PARAMETERS

2.1 INTRODUCTION

If the circuit parameters are varying along the z-axis, the model and the basic formulation must satisfy certain requirements which can be stated as follows: (i) the basic circuit and beam rf-variables must be chosen such that they are continuous along the axis, even if the circuit parameters are discontinuous, (ii) the beam-to-circuit coupling must be appropriately formulated in terms of wavelength-dependent coupling coefficients rather than frequency-dependent coefficients.

The requirement (i) serves to facilitate the mathematical formulation of problems having z-dependence in general. The requirement (ii) is necessary for handling cases of high circuit loss, i.e., attenuators in general. In such cases the wavelength beam-to-circuit coupling is specified by an attenuated and increasingly fast propagation factor entering the argument of the coupling coefficient, which then itself becomes complex. This implies that the coupling is no longer pure capacitive but has a real component as well.

In the polarization model used in the present work both requirements (i) and (ii) stated above are fully accounted for.

2.2 MATHEMATICAL APPROACH

The following is a formal exposition of the mathematical procedure. In the first part of this work, reported earlier, we established the concept of the transmission matrix $\underset{\sim}{T}$ for a uniform helix section. The transmission matrix relates the rf variables at the input and output ends of the uniform section in the following way:

$$\underset{\sim}{a}(z_p) = \underset{\sim}{T}(p) \, \underset{\sim}{a}(z_{p-1}) , \tag{2.1}$$

2

where $\underline{a}(z_p)$ is a column vector containing the rf variables of all the frequency components. The transmission matrix implicitly contains large signal effects, in that the off-diagonal submatrices are nonzero. These represent the nonlinear coupling terms between the various harmonics.

If the circuit parameters vary over a certain length of the TWT, this length is subdivided into a sufficiently large number of subsections. In each of these the parameters are considered to be constant and independent of z.

The over-all transmission matrix for the tapered section is then given by the product of the separate transmission matrices of the p subdivisions.

$$\underline{T} = \underline{T}(p)\ \underline{T}(p-1) \ . \ . \ . \ \underline{T}(2)\ \underline{T}(1) \tag{2.2}$$

The formula applies for the practical computational case in which the number p is finite. The exact formula is

$$\underline{T} = \lim_{p \to \infty} [\underline{T}(p)\ \underline{T}(p-1) \ . \ . \ . \ \underline{T}(2)\ \underline{T}(1)] \tag{2.3}$$

This simply means that the subdivisions have to be made sufficiently small to simulate the real situation. In practice, this is no problem, since the computer program is sufficiently general to accommodate the indicated procedure. It is more a question of organization of input data for the computer.

In the small signal domain, the over-all transmission matrix is diagonal on a submatrix basis, and the computations are correspondingly simple, in that each harmonic components can be treated independently of the others.

3.0 RELATIVISTIC CORRECTIONS

The relativistic corrections that have to be implemented at high dc voltages have been introduced. These corrections are all expressed in terms of the usual relativistic factor γ, defined by:

$$\gamma = \left[1 - \frac{v_0^2}{c^2} \right]^{1/2} \tag{3.1}$$

The relativistic effects appear in the following parts:

1. The relativistically correct dc velocity v_0 is obtained from the dc voltage V_o by:

$$v_0^2 = \frac{1}{2} \frac{e}{m_o} V_0 \frac{1 + \frac{1}{2} \frac{e}{m_0} \frac{V_0}{c^2}}{\left[1 + \frac{e}{m_0} \cdot \frac{V_0}{c^2} \right]^2} \tag{3.2}$$

   The last fraction represents the relativistic correction, being unity if V_0 is small.

2. The <u>longitudinal</u> relativistic mass m_ℓ is increased by the factor $1/\gamma^3$.

$$m_\ell = m_0 \frac{1}{\gamma^3} \tag{3.3}$$

4

3. The <u>transverse</u> relativistic mass m_t is increased by the factor $1/\gamma$.

$$m_t = m_0 \frac{1}{\gamma} \qquad\qquad (3.4)$$

4. The plasma frequency ω_p is reduced by the factor $\gamma^{3/2}$

$$\omega_p = \omega_{p0} \, \gamma^{3/2} \qquad\qquad (3.5)$$

With the indicated corrections introduced into the program at the appropriate places the results are relativistically correct for small signals and approximately correct for large signals.

4.0 FUNDAMENTAL AND SPACE-HARMONIC INTERACTIONS IN THE TWT

The main objective of the present work is to analyze backward wave instabilities. But in order to accomplish this task it has been necessary first to establish a sufficiently detailed physical model together with a sufficiently simple mathematical formulation of the over-all forward and backward interactions taking place in a multisection TWT.

4.1 INTERACTIONS OF BEAM AND CIRCUIT IN THE BACKWARD MODES

It is necessary to distinguish between left- and right-handed helices because of possible inclusions of pitch reversals in the helix structure. The rf fields of left- and right-handed helices are given by the following expansions in space-harmonic components:

$$\vec{E}(\vec{r}, \theta, z) = \sum_{m=-\infty}^{\infty} \vec{E}_m(r) \, e^{-j\beta_m z} \, e^{-jm\theta} \tag{4.1}$$

$$\vec{E}(\vec{r}, \theta, z) = \sum_{m=-\infty}^{\infty} \vec{E}_m(r) \, e^{-j\beta_m z} \, e^{jm\theta}, \tag{4.2}$$

In these expansions the exponent β_m is given by:

$$\beta_m = \beta_0 + \frac{2\pi m}{d} \,, \tag{4.3}$$

where d is the helix pitch.

The dispersion diagrams of the left- and right-handed helices are shown in Figures 4-1 and 4-2, respectively.

The figures labeled a) and b) in these drawings are mirror images of each other. They both exist because the helix looks the same in either direction.

From a study of the diagrams we can draw the following conclusions relating to the basic interactions:

1. For a left-handed helix the backward wave interaction involves the $m = -1$ space harmonics.

2. For a right-handed helix the backward wave interaction involves the $m = +1$ space harmonics.

3. The fundamental mode interaction is not affected by the direction of helix pitch.

4. In a given left- or right-handed helix section only one of the two space harmonics $m = -1$ or $m = +1$ is involved. This is because the $m = -1$ and $m = +1$ harmonics are always in opposite directions. Therefore, only one of the two space-harmonic components can be synchronized with the beam, namely the one with positive propagation constant.

The same considerations do not apply to the corresponding space harmonic components of the beam. If a $m = -1$ mode is excited in the beam through backward wave interaction in a left-handed helix section, this particular beam symmetry is retained through a pitch reversal. In the reversed pitch section the $m = -1$ existing in the beam is completely decoupled from the circuit, because the $m = -1$ circuit mode in the

7
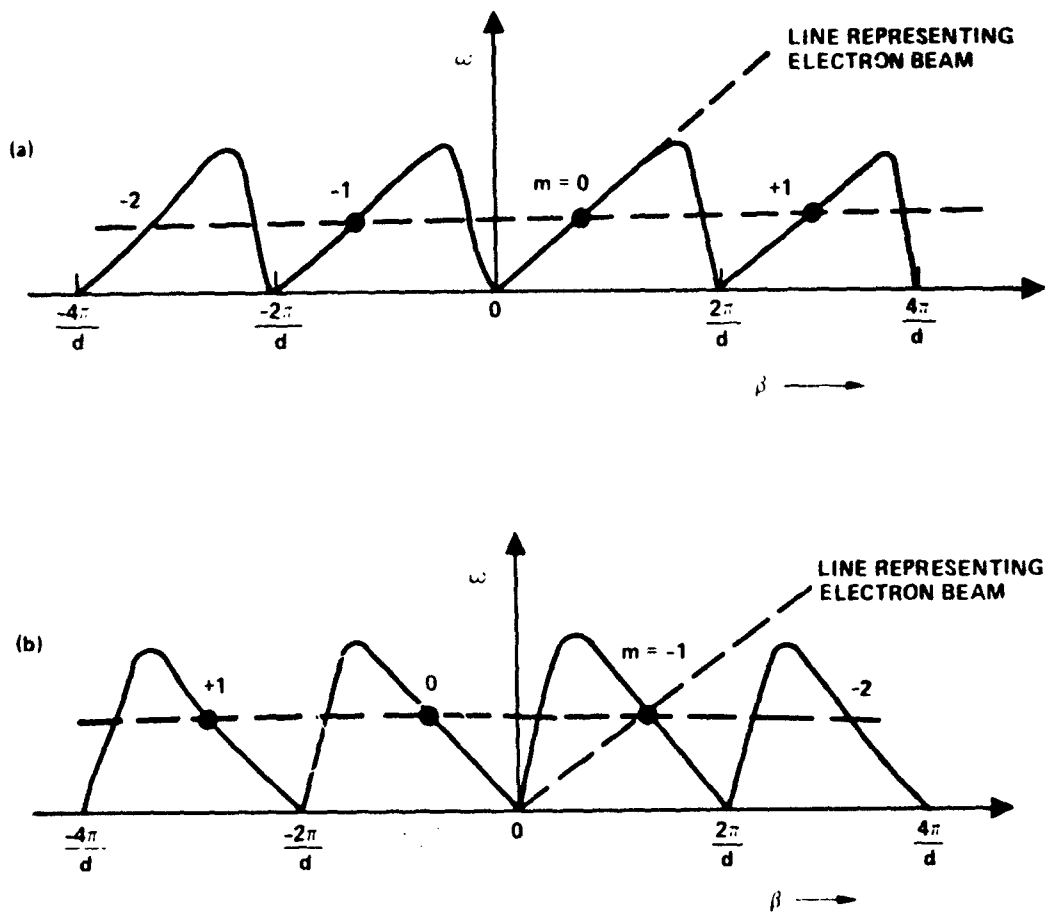
Figure 4-1   Dispersion diagram of left-handed helix.
a)   Forward wave interaction in the
     m = 0 mode
b)   Backward wave interaction in the
     m = -1 mode

8
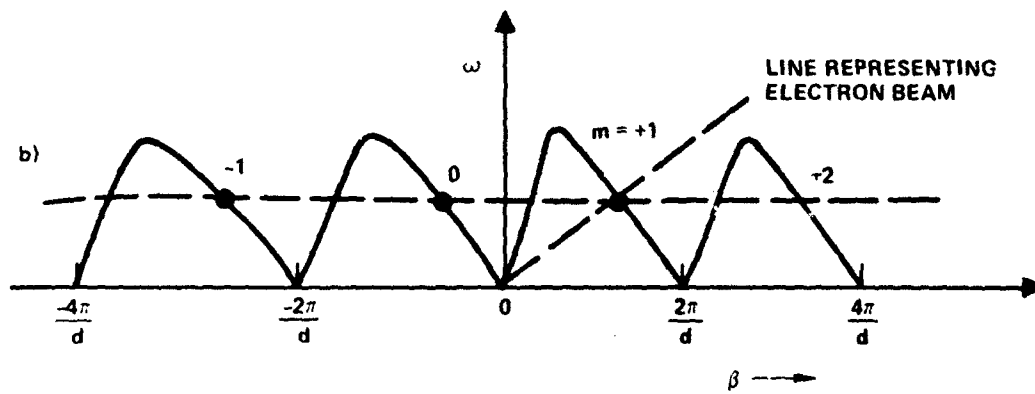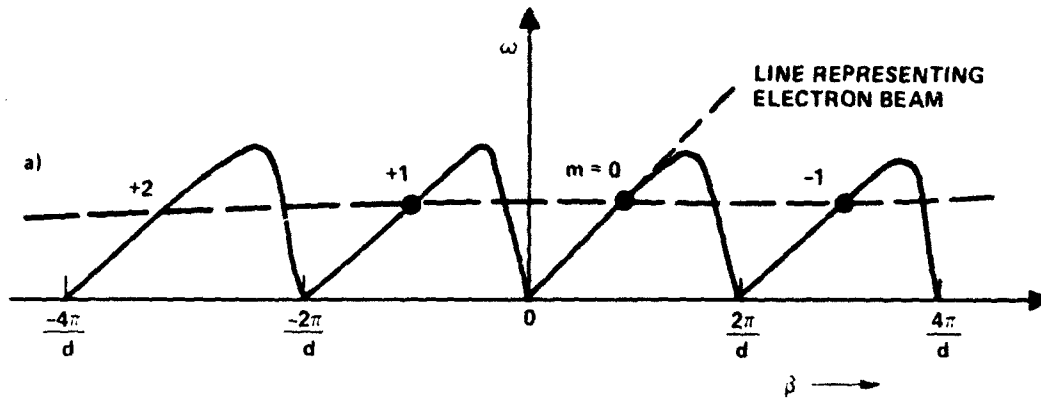
Figure 4-2   Dispersion diagram of right-handed helix.
a)   Forward wave interaction in the
m = 0 mode
b)   Backward wave interaction in the
m = +1 mode

9

right-handed helix is completely out of synchronism with the beam. In such a pitch reversal the effect on the beam is that it suddenly sees a noninteracting circuit, all referred to the m = -1 beam mode.

Conversely, if we started out with a right-handed helix, the m = +1 mode is the appropriate backward mode. A pitch reversal reduces the beam-circuit interaction for the m = +1 mode to essentially zero.

The points brought up here might conceivably be of importance for reduction of backward wave instabilities through pitch reversals. Provided these can be designed with negligible fundamental mode reflections over the appropriate frequency band, they appear to represent a practical possibility. As far as backward wave interactions is concerned the effective length of the helix is reduced by a factor of two, which certainly would serve to diminish the instability problem.

4.2 THE ARCHITECTURE OF FORWARD AND BACKWARD WAVE INTERACTIONS

Using the previous discussion as a guideline let us establish the relevant interactions that need be considered. Figure 4-3 shows a schematic diagram which helps sort out the interactions and the angular symmetries of the modes involved. The first point which we have to keep in mind is that the circuit alone supports two independent modes, one traveling in the forward direction with group velocity $v_g > 0$, and one traveling in the backward direction with $v_g < 0$. The corresponding interactions with the beam are those shown in the lower blocks of Figure 4-3a and 4-3b.

The second point which we must keep in mind is that all circuit harmonics are intimately coupled, so that the excitation of one particular harmonic by the beam, say the m = -1 harmonic shown in Figure 4-3b, automatically gives rise to a proportionate excitation of all the other circuit harmonics.

CIRCUIT FORWARD MODE, $v_g > 0$ ⟶

CIRCUIT ⟶ [-2] ⟷ [-1] ⟷ [m = 0] ⟷ [+1] ⟷ [+2] —

ELECTRON BEAM [m = C] ⟶

(a)

CIRCUIT BACKWARD MODE, $v_g < 0$ ⟵

CIRCUIT ⟶ [-3] ⟷ [-2] ⟷ [-1] ⟷ [m = 0] ⟷ [+1] —

ELECTRON BEAM [m = -1] ⟶

(b)
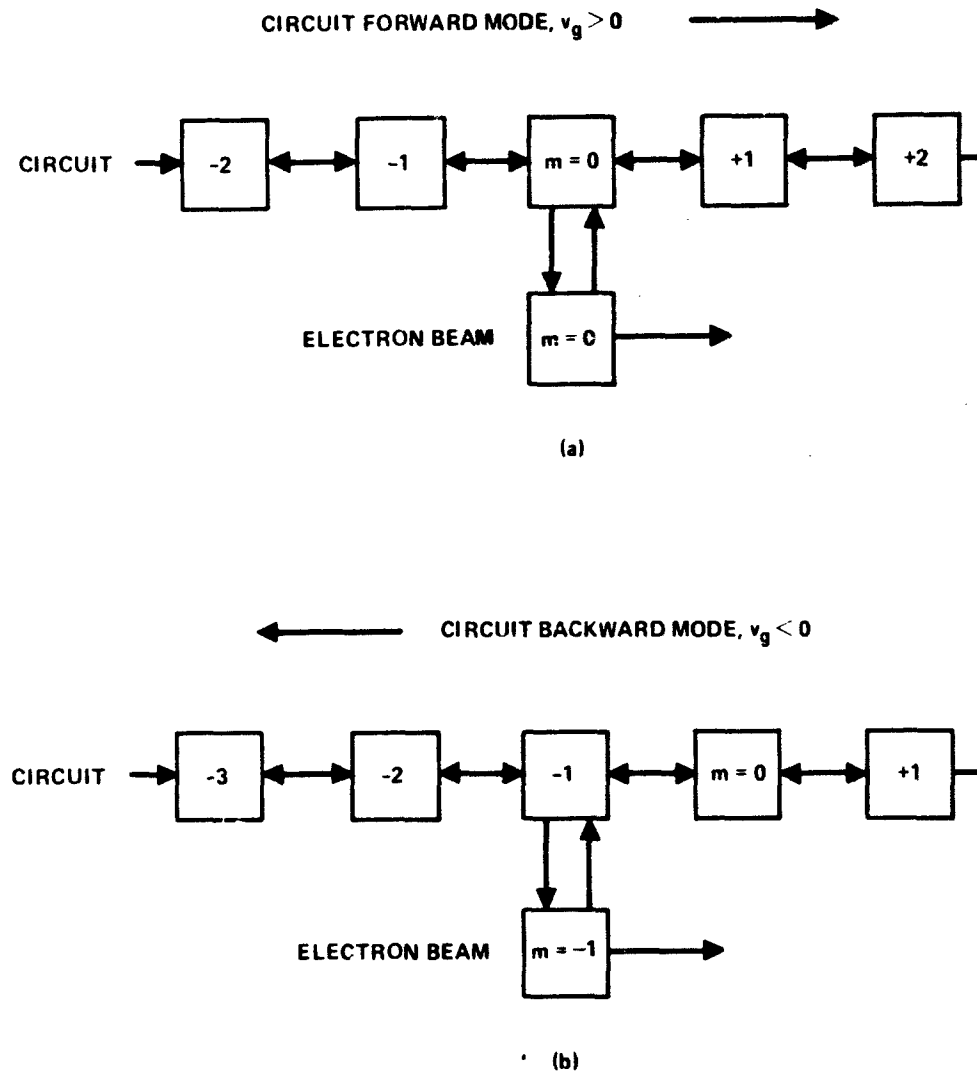
Figure 4-3   Schematic diagram illustrating the circuit and
beam harmonics involved in: a) forward inter-
action, b) backward interaction in a left-
handed helix.

The third point we like to make is that it is convenient to interpret the circuit voltage and circuit current as the fundamental components, i.e., those corresponding to the m = 0 mode, both in forward and backward interactions.

The relevant interactions and rf circuit and beam variables are those summarized in the schematic diagrams of Figures 4-4 and 4-5. The forward interaction shown in Figure 4-4 involves only the circularly symmetric modes m = 0 of the circuit and the beam. The rf variables are the normalized circuit voltage v_f, the circuit current i_f, the normalized beam velocity U_o, and the normalized displacement S_0. This mode of operation is the regular TWT amplification process, which is independent of the direction of pitch.

The backward wave interactions depicted in Figure 4-5 involve the m = ±1 beam and circuit modes, and the m = 0 circuit mode. As stated previously, the relations between the m = 0 and m = ±1 circuit space harmonics are fixed.

4.3   THE MATCHING PROBLEM

With these considerations in mind let us consider the matching problem at some discontinuity along the helix, such as a change in pitch angle. Which rf variables are continuous across the discontinuity, and need be considered? Expressed in general terms, the circuit voltage, circuit current, beam velocity, and beam displacement are continuous. Let us first consider the circuit variables. As noted previously it suffices to express these in terms of the fundamental (m = 0) component, which consists of the sum of the forward components v_f and i_f (Figure 4-4) and the backward traveling components v_b and i_b (Figure 4-5). The latter are also of the m = 0 symmetry, but are caused by interactions of the m = -1 or m = +1 components, depending on the sense of rotation of the helix, as already shown in Figure 4-5.

FORWARD CIRCUIT MODE

v_f

i_f

$m = 0$

CIRCULARLY SYMMETRIC
BEAM MODES

U_0

S_0
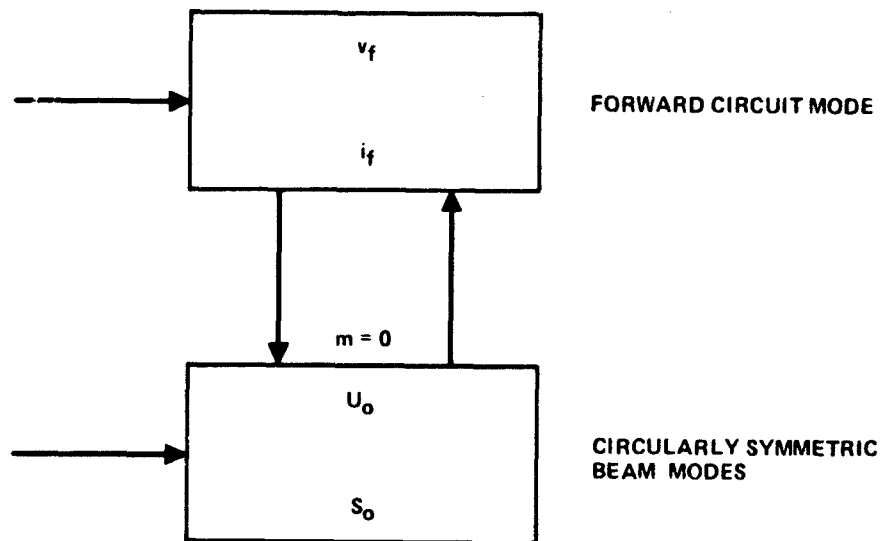
Figure 4-4   Schematic diagram of forward interaction,
and the rf variables involved.

G7548

CIRCUIT VOLTAGE AND CURRENT
FOR LEFT-HANDED HELIX

CIRCUIT VOLTAGE AND CURRENT
FOR RIGHT-HANDED HELIX

m = -1   m = 0   m = +1

v_{-1} $v_{b,-1}$ $v_{b,+1}$ v_{+1} BACKWARD
i_{-1} $i_{b,-1}$ $i_{b,+1}$ i_{+1} CIRCUIT
                                                                   MODE

m = +1   m = +1

U_{-1} U_{+1}
S_{-1} S_{+1}

FORWARD BEAM MODES   FORWARD BEAM MODES
FOR LEFT-HANDED HELIX   FOR RIGHT-HANDED HELIX

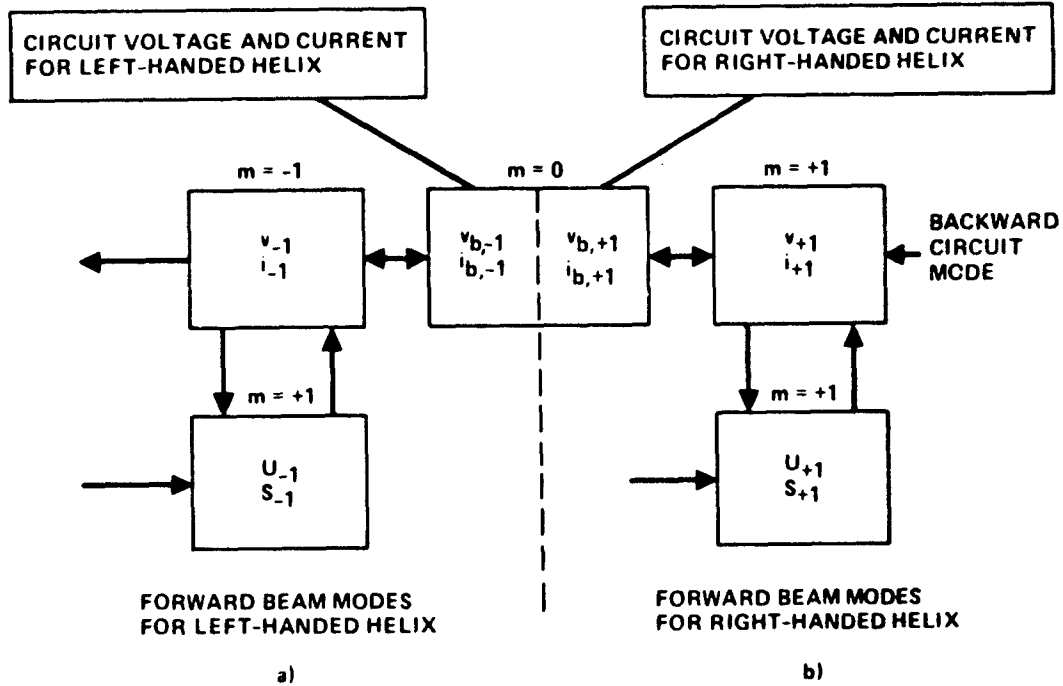a)   b)

Figure 4-5   Schematic diagram of backward interaction,
              and the rf variables involved:
              a)   left-handed helix,
              b)   right-handed helix.

14

The rf variables of the beam corresponding to different m-values are orthogonal, and presumably are not coupled by a change in helix pitch. Accordingly, it is necessary to match the various rf beam variables, corresponding to different m-values, separately. These variables are U_{-1} and S_{-1} for the m = -1 symmetry, U_{+1} and S_{+1} for the m + 1 symmetry, and U_0 and S_0 for the m = 0 symmetry. Altogether we have eight matching conditions of circuit and beam variables. If pitch reversals are not involved at any position along the helix, these are reduced to six conditions.

If the forward mode is disregarded, these six conditions are further reduced to four, namely continuity of:

Backward circuit voltage v_b
Backward circuit current i_b
Beam velocity U_{-1}
Beam displacement S_{-1},
$$(4-4)$$

where we have assumed a left-handed helix.

However, with the forward wave disregarded, there are only three independent wave solutions available. These are the three solutions of the third-order backward wave dispersion relation specifying the coupled beam-circuit system in the backward mode. But this means that we have only three independent equations to determine the four rf variables. Under these circumstances we are left with the only alternative of disregarding one of the rf variables in (4-4), say the beam velocity U_{-1}, and use the other three for matching at the pitch change. This is a procedure which has been used in the past, but is rather questionable, because the forward mode is bound to be subject to some reflections at a discontinuity of pitch angle. Only in the very special case that the circuit impedances on either side of the discontinuity are the same,

will there be no reflections. But this conditions is not likely to occur
in the general case. We are therefore forced to adapt <u>six</u> independent
boundary conditions, and as many as <u>eight</u> conditions if pitch reversals
are involved. The two additional conditions in the latter case arise
because the two <u>independent</u> $m = -1$ and $m = +1$ beam modes are both present,
traveling along the beam and interacting with the appropriate space har-
monic of the left-handed and right-handed helix sections, respectively.

From Figure 4-5 it is noted that in a given helix section, left-handed
or right-handed, only <u>one</u> of the $m = -1$ or $m = +1$ beam-to-circuit inter-
actions is involved. From inspection of the dispersion diagrams shown
earlier in Figures 4-1b and 4-2b we conclude that these are <u>identical</u>.
Hence, the <u>circuit equations</u> of the $m = -1$ and $m = +1$ interactions will
be the same. However, the <u>electronic equations</u> for $m = -1$ and $m = +1$ are
not the same in the general case. Only for confined focusing are they
identical. The physical reason for the difference is the presence of
the dc focusing magnetic field which introduces a nonsymmetric effect
with regard to the positive ($m = 1$) and negative ($m = -1$) angular
dependence. A typical example is the Brillouin focused beam, for which
the propagation factors of the $m = -1$ and $m = +1$ modes are different.

Hence, a section of <u>reversed</u> pitch essentially retains the same circuit
equation, but requires a difficult electronic equation, except for con-
fined flow. The case of confined flow is therefore considerably simpler
to analyze.

4.4 DISPERSION RELATIONS FOR THE FORWARD AND BACKWARD WAVES

A detailed analysis of the coupled circuit and electronic equations leads
to the same form of the dispersion relation for the forward and the
backward waves, i.e., for $m = 0$ and $m = \pm 1$. The relation is expressed
in the matrix form:

$$0 = \begin{bmatrix} -jB_m^{(i)} & , & j\dfrac{l_0}{V_0}Z_{cm}\left(\dfrac{v_0}{v_{cm}}\right)\kappa_m & \Bigg| & 0 & , & 0 \\[2em] j\left(\dfrac{v_0}{v_{cm}}\right)\dfrac{V_0}{I_0 Z_{cm}} & , & -jB_m^{(i)} & \Bigg| & 0 & , & -B_m^{(i)}f_m^{(i)} \\[1em] \hline \\ \dfrac{1}{2}jB_m^{(i)}f_m^{(i)} & , & 0 & \Bigg| & j\left(1-B_m^{(i)}\right), & & \dfrac{2}{p}R_m^{(i)2} \\[2em] 0 & , & 0 & \Bigg| & -1 & , & j\left(1-B_m^{(i)}\right) \end{bmatrix} q_m^{(i)}$$

$$i = 1,2,3$$
$$m = 0, \pm 1$$

$$(4.5)$$

The parameters appearing in the equation are the following:

$$B_m^{(i)} = \frac{\beta_m^{(i)}}{\beta_e} = \text{normalized propagation factors of the three}$$
$$\text{modes, corresponding to } i = 1,2,3$$

$$R_m^{(i)} = \text{plasma reduction factors for the same modes}$$

$$f_m^{(i)} = \text{coupling coefficients for the same modes}$$

$$v_{cm} = \text{phase velocity of the circuit for the mth space harmonic}$$

$$Z_{cm} = \text{circuit impedance of the mth harmonics}$$

$$\kappa_m = 1 - j(-1)^m \frac{R_0}{\beta_{c0}Z_{c0}} = \text{loss parameter}$$

17

$$\Omega_p = \frac{\omega_p}{\omega} = \text{normalized plasma frequency}$$

In (4.5) the column $q_m^{(i)}$ is the <u>state vector</u> of the particular mode

$$q_m^{(i)} = \begin{bmatrix} \dfrac{-2j}{B_m^{(i)} f_m^{(i)}} \left[\left(1 - B_m^{(i)}\right) - \Omega_p^2 R_m^{(i)^2} \right] \\[2em] \dfrac{-2j}{\dfrac{I_0}{V_0} \, cm \left(\dfrac{v_0}{v_{cm}}\right) \kappa_m f_m^{(i)}} \left[\left(1 - B_m^{(i)}\right)^2 - \Omega_p^2 R_m^{(i)^2} \right] \\[2em] j \left(1 - B_m^{(i)}\right) \\[1em] 1 \end{bmatrix} \qquad (4.6)$$

$$i = 1,2,3$$
$$m = 0, \pm 1$$

The state <u>matrix</u> is constructed from the state vectors by

$$Q_m = \begin{bmatrix} q_m^{(1)} & q_m^{(2)} & q_m^{(3)} \end{bmatrix}_{m = 0, \pm 1} \qquad (4.7)$$

The rf variables of mode m are then specified by the relations

$$a_m(z_0) = \begin{bmatrix} v_m(z_0) \\ i_m(z_0) \\ U_m(z_0) \\ S_m(z_0) \end{bmatrix} = Q_m \, e^{-jD_m z_0} A_m, \qquad (4.8)$$

$$m = 0, \pm 1$$

18

Where $\underset{\sim}{D}_m$ is a diagonal matrix containing the three propagation factors of the mode m.

These are obtained from the determinantal equation associated with (4.5)

$$\Delta_m = 0 \qquad m = 0, \pm 1 \qquad (4.9)$$

Furthermore, the vector $\underset{\sim}{A}_m$ in (4.8) contains the normal mode amplitudes of the three component modes, which are independent of the axial coordinate z_0 within a uniform helix section. But they undergo changes at any discontinuity of the helix.

ith reference to the variables listed after (4.5) one should note that:

1. The plasma reduction factors and the coupling coefficients are not the same for the m = 0 and the m = ±i modes.

2. The circuit impedance Z_{cm} is positive for forward mode m = 0 and negative for the backward modes m = ±1.

3. The loss parameters κ_m is the same for m = 0 and m = ±1 except for the sign of the imaginary part.

With these restrictions the same general equations apply to all three modes m = 0, and m = ±1. Note that in this formulation all the modes have <u>positive</u> propagation constants $B_m^{(i)}$, because the phase velocities are all positive. The circuit part of the m = ±1 modes relate to the <u>space-harmonic</u> voltage and current $v_{\pm 1}$ and $i_{\pm 1}$, appearing in (4.8). In the next step one must convert from these variables to the corresponding <u>fundamental</u> components v_b and i_b appearing in the diagrams of Figure 4-5.

4.5 SPECIFICATION OF THE RF VARIABLES IN THE BACKWARD TRAVELING WAVE

In view of the strongly coupled space harmonics of the helix this procedure is fairly straightforward. Let us first look at the propagation factor of the m = 0 backward traveling mode. From the general formula (4.3) we obtain

$$B_{0,backward}^{(i)} = B_b^{(i)} = B_m^{(i)} - \frac{2\pi}{\beta_e a},$$
(4.10)

where $\beta_e d$ is the normalized helix pitch.

The corresponding backward circuit voltage of the fundamental component is obtained by noting that the **total** rf circuit power P in all harmonics is given by the formula

$$|z_{cm}| = \frac{|v_m|^2}{2P} \qquad m = 0, \pm 1, \pm 2, \ldots$$
(4.11)

Hence

$$\left|\frac{v_m}{v_b}\right|^2 = \left|\frac{z_{cm}}{z_{co}}\right|$$

or

$$v_b = v_m \sqrt{\left|\frac{z_{co}}{z_{cm}}\right|} \qquad m = \pm 1 \quad ,$$
(4.12)

which relates the normalized rf voltages of the m = 0 mode and the m = ±1 modes.

The inverse relation applies to the corresponding rf currents. Since

$$i_b = -\frac{v_b}{Z_{co}}\frac{V_o}{I_o}$$

(4.13)

$$i_m = \frac{v_m}{Z_{cm}}\frac{V_o}{I_o} \quad ,$$

we obtain

$$i_b = i_m\sqrt{\left|\frac{Z_{cm}}{Z_{c0}}\right|} \qquad\qquad m = \pm 1 \qquad (4.14)$$

In this backward mode Z_{c0} as well as Z_{cm} must be taken negative, but we have used absolute signs in (4.12) and (4.14) in order to avoid errors.

Using the established relations (4.10)-(4.14) between the $m = 0$ and $m = \pm 1$ components in the backward mode, the relevant rf variables for this mode, to be used in the matching procedure, are specified by the relation:

$$\underset{\sim}{a}_b(z_0) = \begin{bmatrix} v_b(z_0) \\ i_b(z_0) \\ U_m(z_0) \\ S_m(z_0) \end{bmatrix} = \underset{\sim}{Q}'_m e^{-j\underset{\sim}{D}_m z_0} \underset{\sim}{A}_m \quad , \qquad (4.15)$$

where the modified state matrix $\underset{\sim}{Q}'_m$ is given in terms of the original $\underset{\sim}{Q}_m$ by:

21

$$
\underline{Q}'_m = \begin{bmatrix}
\sqrt{\left|\dfrac{Z_{c0}}{Z_{cm}}\right|}\, e^{j|m|2\pi/\beta_e d} & , & 0, & 0 & , & 0 \\[20pt]
0 & , & \left|\dfrac{Z_{cm}}{Z_{c0}}\right|\, e^{j|m|2\pi/\beta_e d} & , & 0 & , & 0 \\[20pt]
0 & , & 0, & 1 & , & 0 \\[20pt]
0 & , & 0, & 0 & , & 1
\end{bmatrix} \underline{Q}_m
$$

$$m = 0, \pm 1$$

$$(4.16)$$

By the described procedure we have been able to express the rf variables of the backward traveling wave in the form (4.15) which involves the $m = 0$ circuit rf variables. This is a necessary step in the matching process, as discussed earlier.

Before concluding this section on the backward traveling wave we must pay proper attention to the discrimination of left- and right-handed helices. In light of the earlier discussions it follows that the $m = +1$ and $m = -1$ waves do not simultaneously exist with their full range of composite mode solutions, described by the superscript i. The full set corresponds to three modes, with i = 1, i = 2, and i = 3, respectively. But either the $m = +1$ or the $m = -1$ wave has only <u>two</u> composite modes. The reason for this is that one of the two $m = \pm 1$ set of beam waves, both of which have about the same phase velocity, is way out of synchronism with the corresponding space harmonic component of the circuit. We can easily convince ourselves that this is the case by studying the circuit dispersion diagrams of Figures 4-1b and 4-2b. Hence, for either $m = +1$ or $m = -1$, the interaction with the circuit

22

disappears, leaving us with the two decoupled space charge modes corresponding to the particular noninteracting m - value.

More specifically, for a left-handed helix the m = +1 circuit space harmonic is way out of synchronism with the beam (see Figure 4-1b) and, therefore, the m = +1 space charge waves are completely decoupled from the circuit. Hence, in the left-handed helix section only two modes corresponding to m = +1 exist. Conversely, in a right-handed section there are only two modes associated with the m = -1 wave.

These considerations imply that in any one helix section we have a total of eight independent normal mode amplitudes, which will be discussed in more detail in the next section.

4.6 SUMMARY OF NORMAL MODE AMPLITUDES

In general, the normal-mode amplitudes refer to the independent and arbitrary components in the normal mode vector $\underline{A}_m$, appearing in (4.8) and (4.15). In this form they are arbitrary, because the normal mode solutions have not yet been matched at the discontinuities between the helix sections. In effect, the matching procedure provides exactly sufficient conditions to determine the normal mode amplitudes everywhere.

Let us specify explicitly the independent normal modes in left-handed and right-handed helix sections, respectively.

4.6.1 Left-Handed Helix

The fundamental forward wave has three independent modes, corresponding to m = 0 and i' = 1, 2, and 3. The backward wave has three independent solutions corresponding to m = -1, and two solutions corresponding to m = +1. The eight independent mode amplitudes can be summarized as follows:

$$m = 0: \qquad A_0^{(1)} \qquad A_0^{(2)} \qquad A_0^{(3)} \qquad (4.17)$$

$$m = -1: \qquad A_{-1}^{(1)} \qquad A_{-1}^{(2)} \qquad A_{-1}^{(3)} \qquad (4.18)$$

$$m = +1: \qquad A_{+1}^{(1)} \qquad A_{+1}^{(2)} \qquad (4.19)$$

4.6.2 Right-Handed Helix

In this case the corresponding normal mode amplitudes are:

$$m = 0: \qquad A_0^{(1)} \qquad A_0^{(2)} \qquad A_0^{(3)} \qquad (4.20)$$

$$m = -1: \qquad A_{-1}^{(1)} \qquad A_{-1}^{(2)} \qquad (4.21)$$

$$m = +1: \qquad A_{+1}^{(1)} \qquad A_{+1}^{(2)} \qquad A_{+1}^{(3)} \qquad (4.22)$$

4.7 COMPACT FORMULATION OF THE FULL SET OF RF EQUATIONS

From the foregoing discussion it is quite apparent that the matching of
eight normal-mode amplitudes at the intersections between different helix
sections is a fairly complex mathematical task. It can best be accom-
plished by etablishing a systematic 8-dimensional matrix formalism.

For convenience and clarity of the exposition let us introduce sub-
matrices in the state matrix $\underset{\sim}{Q}_m'$ defined by (4.16), (4.6), and (4.7).
Let

$$
\underset{\sim}{Q'_m} = \left[\begin{array}{c} \underset{\sim}{P_m} \\ - - - - \\ \underset{\sim}{W_m} \end{array} \right] \begin{array}{c} \} \ 2 \\ \\ \} \ 2 \end{array} \qquad\qquad (4.23)
$$

$$
\underbrace{}_{3} \qquad\qquad m = 0, \pm 1
$$

As indicated in (4.23) $\underset{\sim}{P_m}$ and $\underset{\sim}{W_m}$ are 3 x 2 submatrices, except for the decoupled modes corresponding to (4.19) and (4.21). In the latter case $\underset{\sim}{P_m}$ and $\underset{\sim}{W_m}$ are 2 x 2 submatrices.

We can now proceed to use (4.8) and (4.15) for the various waves and modes and construct matrix relations for the over-all eight rf variables in a particular section. These look a bit different for the left-handed and right-handed sections.

4.7.1 Left-Handed Helix Section

The following matrix relation applies:

$$(4.24)$$

The left column specifies all the eight rf variables involved in the left-handed helix section. The first 8 x 8 matrix on the right is a generalized state matrix for the over-all system. The second 8 x 8 matrix is the diagonal exponential matrix containing all the eight propagation factors, and the last column represents the eight independent normal mode amplitudes. Equation (4.24) is an extension of (4.8) from four dimensions to eight dimensions. The shaded blocks in the equation correspond to the noninteracting $m = +1$ space charge waves.

4.7.2 Right-Handed Helix Section

The corresponding relation for the right-handed section is the following:

$$(4.25)$$

Equations (4.24) and (4.25) form the very basis of the analysis of backward wave instabilities in multisection TWTs. All the elements in the 8 x 8 matrices are known from the specified data and evaluation of the previously stated equations.

It has been common practice in the past to analyze backward wave instabilities using various simplifications in the model and in the mathematical procedure. Most of these approximations are justified only by the ensuing mathematical simplifications and tractability, and are not justified from physical reasoning. The more common approximations can be easily obtained from the general formulae above. Let us have a look at these.

4.8 SPECIAL CASES AND APPROXIMATIONS

If there are no pitch reversals along the entire helix structure, only one of the two m = ±1 space harmonics is involved in the interaction. Let us assume that the helix is left-handed, in which case (4.24) applies. In this case the m = +1 wave can not be excited in any section and is therefore nonexistent. Hence, the corresponding normal mode amplitudes specified by A_{+1} are zero everywhere.

$$A_{+1} \equiv 0 \qquad\qquad (4.26)$$

These two modes are the decoupled space charge modes which had to be excited in some other right-handed section. But since these do not exist, the modes are nonexistent. In (4.24) these are represented by the last two equations, corresponding to the shaded areas. By removing all the shaded blocks, the resulting equation becomes of sixth order, and represent an exclusive left-handed helix TWT.

Similarly, if all sections are right-handed, the m = -1 waves are not excited, in which case:

$$\underset{\sim}{A}_{-1} \equiv 0 \tag{4.27}$$

The relevant equation is now (4.25) with all the shaded blocks removed.

Inspection of (4.24) and (4.25) after removal of shaded blocks show that both take exactly the same form:

$$
\begin{bmatrix}
v_0(z_0) \\
i_0(z_0) \\
\hline
U_0(z_0) \\
S_0(z_0) \\
\hline
U_{-1}(z_0) \\
S_{-1}(z_0)
\end{bmatrix}
=
\begin{bmatrix}
\underset{\sim}{P}_0 & \underset{\sim}{P}_{-1} \\
\hline
\underset{\sim}{W}_0 & \underset{\sim}{0} \\
\hline
\underset{\sim}{0} & \underset{\sim}{W}_{-1}
\end{bmatrix}
\begin{bmatrix}
e^{-j\underset{\sim}{D}_0 z_0} & \underset{\sim}{0} \\
\hline
\underset{\sim}{0} & e^{-j\underset{\sim}{D}_{-1} z_0}
\end{bmatrix}
\begin{bmatrix}
\underset{\sim}{A}_0 \\
\hline
\underset{\sim}{A}_{-1}
\end{bmatrix}
\tag{4.27}
$$

(column headers: 3, 3, 3, 3; row brackets: } 3, } 3)

forward wave column — backward wave column

Even if the equations are the same **form** for left-handed and right-handed helices, the elements in the matrices are not the same for m = -1 and m = +1. They are the same only for confined flow, but not for general balanced beams, including Brillouin-beams. These more subtle points were discussed earlier.

Backward wave instabilities are often analyzed disregarding the forward
traveling wave. This is legitimate if there are no discontinuities in
the form of pitch changes along the helix. However, the use of this
approximation for analyzing the effect of discontinuous changes in
pitch angle is very questionable, and at best gives a crude approxima-
tion to the starting condition.

However, for the sake of completeness, let us discuss how this approxi-
mation follows from (4.27) by putting the forward traveling wave ampli-
tude $\underset{\sim}{A}_0$ equal to zero.

$$\underset{\sim}{A}_0 = 0 \qquad (4.28)$$

Hereby, (4.27) is simplified to:

$$
\begin{bmatrix}
v_0(z_0) \\
i_0(z_0) \\
- - - - \\
U_{\pm 1}(z_0) \\
S_{\pm 1}(z_0)
\end{bmatrix}
=
\begin{bmatrix}
\underset{\sim}{P}_{\cdot 1} \\
- - - - \\
\underset{\sim}{W}_{\cdot 1}
\end{bmatrix}
e^{-j\underset{\sim}{D}_{\pm 1} z_0} \underset{\sim}{A}_{\pm 1}
\qquad (4.29)
$$

which is just the same as the original equation (4.15).

In the present work we shall not use any of the approximations dis-
cussed here, but retain generality by applying (4.24) and (4.25).

4.9 THE TRANSMISSION MATRIX OF A UNIFORM HELIX SECTION

The introduction of transmission matrices for the sections is particu-
larly convenient for the purpose we have in mind.

29

First, let us write (4.24) and (4.25) in the following compact forms:

$$\underline{b}(z_0) = \underline{\underline{M}}_\ell \, e^{-j\underline{\underline{D}}_e z_0} \, \underline{A}_i$$ (4.30)

$$\underline{b}(z_0) = \underline{\underline{M}}_r \, e^{-j\underline{\underline{D}}_r z_0} \, \underline{A}_r \, .$$ (4.31)

where the meanings of the terms follow from comparison with (4.24) and (4.25). Since both equations are of the same form, we can drop the subscripts ℓ and r and simply write:

$$\underline{b}(z_0) = \underline{\underline{M}} \, e^{-j\underline{\underline{D}} z_0} \, \underline{A}$$ (4.32)

The proper subscript can be added once the pitch direction has been specified.

Let us consider the uniform helix section shown in Figure 4-6 and apply (4.32) at both ends of the section. Recalling that the normal mode vector $\underline{A}$ is constant and independent of z_0 within the uniform section, we find, by elimination of $\underline{A}$ from the two equations:

$$\underline{b}(z_{02}) = \underline{\underline{M}} \, e^{-j\underline{\underline{D}}L} \, \underline{\underline{M}}^{-1} \, \underline{b}(z_{01}) \, ,$$ (4.33)

where

$$L = z_{02} - z_{01}$$ (4.34)

The equation is in _transmission_ form, specifying _all_ the rf variables $\underline{b}(z_{02})$ at the output end by the rf variables $\underline{b}(z_{01})$ at the input end of the section. The transmission matrix $\underline{\underline{T}}$ is given by
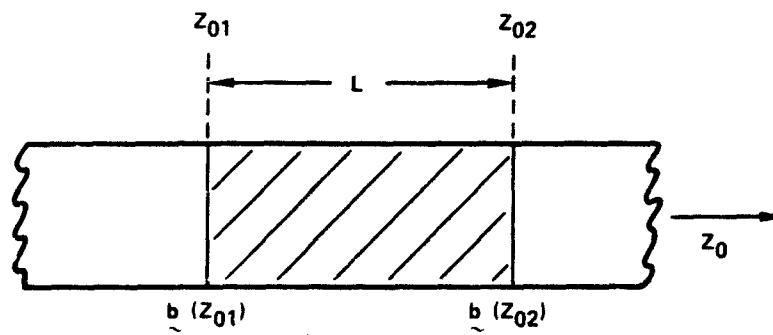
Figure 4-6   Schematic illustration of one
uniform helix section.

$$\underset{\sim}{T} = \underset{\sim}{M} e^{-jDL} \underset{\sim}{M}^{-1} \qquad (4.35)$$

Hence, (4.33) takes the simple form

$$\underset{\sim}{b}(z_{02}) = \underset{\sim}{T} \underset{\sim}{b}(z_{01}) \qquad (4.36)$$

We have also use for the inverse relation

$$\underset{\sim}{b}(z_{01}) = \underset{\sim}{T}^{-1} \underset{\sim}{b}(z_{02}) = \underset{\sim}{I} \underset{\sim}{b}(z_{02}) \qquad (4.37)$$

where

$$\underset{\sim}{I} = \underset{\sim}{T}^{-1} \qquad (4.38)$$

is the inverse transmission matrix.

4.10 THE OVER-ALL TRANSMISSION MATRIX OF THE MULTISECTION TWT

By the transmission matrix formulation (4.35) we have established the
necessary tools for a conceptually simple and mathematically elegant
description of a multisection TWT. The configuration is shown
schematically in Figure 4-7. For each of the N sections the trans-
mission relation (4.36) applies. Some of the sections may be left-
handed and some right-handed, and care must be taken to apply the cor-
responding version of the transmission matrix, evaluated either from
(4.30) or (4.31), in conjunction with (4.35).

As noted earlier, all the rf variables, represented by the columns $\underset{\sim}{b}(z_{01})$
and $\underset{\sim}{b}(z_{02})$ in (4.36) are continuous across the intersections. The
transmission properties, expressed by this equation, can therefore
easily be extended to comprise any number of sections, and in particular,
the full length of the tube. The following result is obtained:
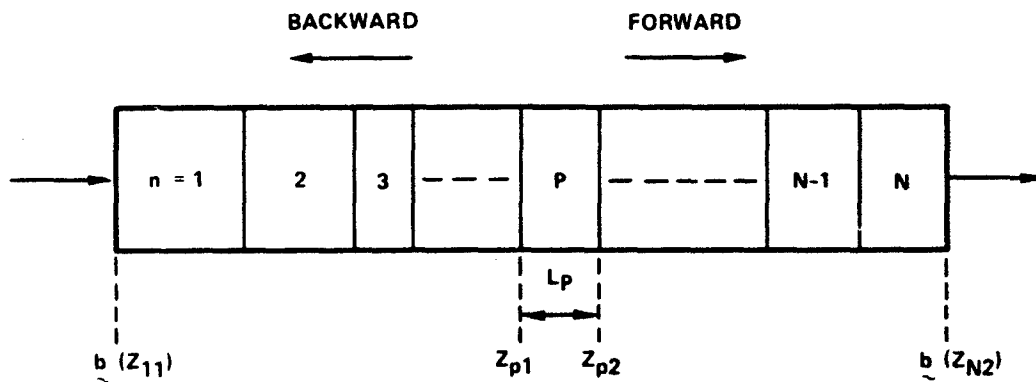
Figure 4-7   Schematic configuration of a multisection TWT
consisting of a total of n uniform, but
different sections.

$$\underset{\sim}{b}(z_{n2}) = \underset{\sim}{T}_n \underset{\sim}{T}_{n-1} \cdots \underset{\sim}{T}_2 \underset{\sim}{T}_1 \, \underset{\sim}{b}(z_{11}) \, , \qquad (4.39)$$

where $\underset{\sim}{b}(z_{n2})$ refers to the output end of the last section, and $\underset{\sim}{b}(z_{11})$ to the input end of the first section. If we write (4.39) in the form

$$\underset{\sim}{b}(z_{n2}) = \underset{\sim}{T} \, \underset{\sim}{b}(z_{11}) \qquad (4.40)$$

the over-all transmission matrix $\underset{\sim}{T}$ is given by the product of all the section transmission matrices

$$\underset{\sim}{T} = \underset{\sim}{T}_n \underset{\sim}{T}_{n-1} \cdots \underset{\sim}{T}_2 \underset{\sim}{T}_1 \qquad (4.41)$$

The transmission relation expressed in (4.40) is a complete and detailed description of the TWT characteristics, including forward gain and backward wave properties. All the elements of the transmission matrix $\underset{\sim}{T}$ can be specified or evaluated from the detailed relations in the earlier part of this report. In the next section we shall show that only _four_ of these are necessary for describing two-port terminal relations.

4.11 TWO-PORT TERMINAL DESCRIPTION OF THE MULTISECTION TWT

Let us express the transmission relation (4.40) in the following more explicit and detailed form:

$$
b(z_{n2}) = \begin{bmatrix} v_0(z_{n2}) \\ i_0(z_{n2}) \\ \hline U_0(z_{n2}) \\ S_0(z_{n2}) \\ U_{-1}(z_{n2}) \\ S_{-1}(z_{n2}) \\ U_{+1}(z_{n2}) \\ S_{+1}(z_{n2}) \end{bmatrix} = \begin{bmatrix} \overbrace{}^{2} & \overbrace{}^{6} \\ \underline{T}_{11} & \underline{T}_{12} \\ \hline \underline{T}_{21} & \underline{T}_{22} \end{bmatrix} \begin{bmatrix} v_0(z_{11}) \\ i_0(z_{11}) \\ \hline U_0(z_{11}) \\ S_0(z_{11}) \\ U_{-1}(z_{11}) \\ S_{-1}(z_{11}) \\ U_{+1}(z_{11}) \\ S_{+1}(z_{11}) \end{bmatrix}
$$

(4.42)

Let us define the _circuit_ column $b_c(z_0)$ and the _beam_ column by $b_e(z_0)$, wher z_0 can be either z_{n2} or z_{11}.

$$
b_c(z_0) = \begin{bmatrix} v_0(z_0) \\ i_0(z_0) \end{bmatrix}
$$

(4.43)

35

$$
b_e(z_0) = \begin{bmatrix} U_0(z_0) \\[2ex] S_0(z_0) \\[2ex] U_{-1}(z_0) \\[2ex] S_{-1}(z_0) \\[2ex] U_{+1}(z_0) \\[2ex] S_{+1}(z_0) \end{bmatrix}
\tag{4.44}
$$

Equation (4.42) can then be subdivided into two component equations:

$$
\underset{\sim}{b}_c(z_{n2}) = \underset{\sim}{T}_{11}\, \underset{\sim}{b}_c(z_{11}) + \underset{\sim}{T}_{12}\, b_e(z_{11})
\tag{4.45}
$$

$$
b_e(z_{n2}) = \underset{\sim}{T}_{21}\, \underset{\sim}{b}_c(z_{11}) + \underset{\sim}{T}_{22}\, b_e(z_{11})
\tag{4.46}
$$

But at the __input__ end all the rf variables in the beam are identically zero, because the beam enters the helix unmodulated. Hence, the corresponding vector $\underline{b}_e(z_{11})$ is identically zero.

$$
b_e(z_{11}) = 0 \, ,
\tag{4.47}
$$

and (4.45) and (4.46) simplify to:

$$
\underset{\sim}{b}_c(z_{n2}) = \underset{\sim}{T}_{11}\, \underset{\sim}{b}_c(z_{11})
\tag{4.48}
$$

$$
b_e(z_{n2}) = T_{21}\, b_c(z_{11})
\tag{4.49}
$$

36

As a consequence of the fact that the rf beam modulations are zero at the input end of the tube, we have been able to obtain nice separate trans-mission matrices for the circuit variables b_c and the beam variables b_e. Of these, the circuit relation (4.48) is by far of most significance, and we shall not use (4.49) any further.

It is quite remarkable that a simple relation like (4.48) describes all the small signal terminal properties of the multisection TWT, including forward gain characteristics and backward wave instabilities. All these properties are contained in the 2 x 2 transmission matrix T_{11}, which is known from the computer calculations of the over-all transmission matrix T.

Hence, the discussions of TWT properties are reduced to a discussion of the properties of the submatrix T_{11}. Only in the simplest cases, and certainly not for multisection TWTs, can we obtain exact or approximate analytical expressions for the elements of T_{11}. But for the computer, determination of T_{11} is a well defined problem and a straightforward procedure using the general formula (4.41).

5.0 BACKWARD WAVE INSTABILITIES

From this base on we can proceed to determine the conditions for backward wave instabilities which are contained in the properties of the T_{11} matrix in (4.48). Let us express the matrix explicitly by its elements:

$$T_{11} = \underset{\sim}{\chi} = \begin{bmatrix} \chi_{11} & \chi_{12} \\ \chi_{21} & \chi_{22} \end{bmatrix}, \tag{5.1}$$

and remember the relevant equation (4.48), repeated here for convenience:

$$\underset{\sim}{b}_c(z_{n2}) = \underset{\sim}{\chi} \, \underset{\sim}{b}_c(z_{11}) \tag{5.2}$$

5.1 THE INHERENT BACKWARD WAVE INSTABILITY

The usual argument for determining backward wave instabilities is the following: If the rf circuit variables $\underset{\sim}{b}_c(z_{n2})$ are zero at the output end, but nonzero at the input end, i.e., $\underset{\sim}{b}_c(z_{11}) \neq 0$, then the backward gain is infinite and the solution unstable, giving rise to oscillations at some frequency. This condition is easily obtained from (5.2) by putting $\underset{\sim}{b}_c(z_{n2}) \equiv 0$, which results in the equation:

$$\underset{\sim}{\chi} \, \underset{\sim}{b}_c(z_{11}) = 0 \tag{5.3}$$

The solution of this homogeneous set of equations specifies the condition for backward wave instabilities. In order for $\underset{\sim}{b}_c(z_{11})$ to be nonzero, the determinant of (5.3) must be zero

$$|\chi| = \chi_{11}\chi_{22} - \chi_{12}\chi_{21} = 0 , \tag{5.4}$$

which is the instability criterion.

The elements in the λ-matrix are functions of all the relevant parameters of the multisection TWT. It reflects the properties of all the sections as far as fixed <u>design</u> parameters are concerned, such as helix impedances, pitch angles, etc. Moreover, λ is also a function of <u>operational</u> parameters, in particular the dc beam current and the frequency ω. We are not at liberty to specify the <u>oscillation frequency</u> $\underline{\omega}$, which is an unknown parameter together with the <u>starting current</u> I_{os}.

Since all the elements in the λ-matrix are <u>complete</u> quantities, the determinantal equation (5.4) contains two independent equations, representing the real and imaginary parts:

$$\left| \lambda(\omega, I_0) \right|_r = 0 \tag{5.5}$$

$$\left| \lambda(\omega, I_0) \right|_i = 0 \tag{5.6}$$

These two equations define implicitly two functional relationships between I_0 and ω, which have to be satisfied <u>simultaneously</u>. In Figure 5-1 these two relations are represented by the intersecting curves in the $\omega - I_0$ plane. The intersection is specified by point A in the diagram and represents the starting current I_{0s} and oscillation frequency ω_s for backward wave instabilities.

The numerical procedure would involve appropriate search routines for determining the intersection point A between the two curves.

At this stage it is appropriate to point out some common errors made in determining the starting current. It is not unusual that the

39

starting condition is established by considering only one equation, say (5.5), or some linear combination of (5.5) and (5.6). Regardless of details, the point is that only one relation between I_0 and ω is specified. In Figure 5-1 this would correspond to disregarding one of the two curves, say the one corresponding to $|\chi(\omega_0,I_0)|_i = 0$. In this erroneous procedure one is then plotting the remaining curve, which in this example would be $|\chi(\omega,I_0)|_r = 0$, and specifying the starting condition as the minimum of the curve. In this example this would be point B, corresponding to an alleged, but incorrect starting current I'_{0s} and frequency ω'_s.

But even if we avoid this incorrect procedure, the described method using both equations (5.5) and (5.6) is not the best way of approaching the instability problem. It is sure that the method gives the correct starting condition for the inherent backward wave instability, which has to do with internal feed-back loops in the circuit-beam system. However, the method is unable to cope with more general configurations characterized by additional feedback from reflections at the input and output terminals. Expressed differently, the described procedure is valid only for perfectly matched input and output terminals. The reason for this deficiency is that the relation (5.2) is not yet expressed in terms of its forward and backward traveling rf components and the corresponding forward and backward gain. In the following we shall develop a procedure along these lines, and arrive at a better method for determination of backward wave instabilities.

5.2 RESOLUTION IN FORWARD AND BACKWARD COMPONENTS IN THE OVER-ALL TRANSMISSION SYSTEM

As already pointed out, the χ-matrix in (5.2) contains all the information on the terminal behavior of the multisection TWT. An equivalent way of expressing this fact is the statement that the behavior is described by the eigenvalues and eigenvectors of χ.
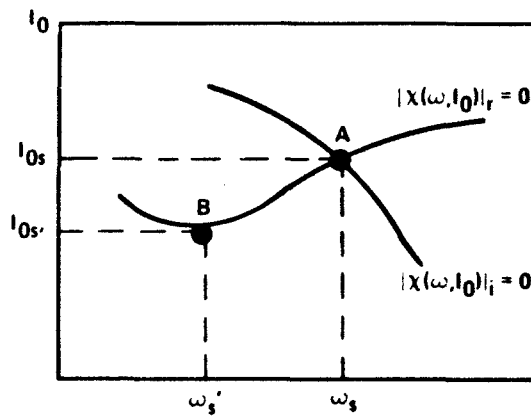
Figure 5-1 Illustration of instability diagram for
backward wave oscillations.

The eigenvalue relation is given by:

$$\underset{\sim}{x}\underset{\sim}{r}_i = \gamma_i \underset{\sim}{r}_i \quad , \quad i = 1, 2 \tag{5.7}$$

Nonzero solutions of $\underset{\sim}{r}_i$ requires the determinant to be zero.

$$| \underset{\sim}{x} - \gamma_i \underset{\sim}{1} | = 0 \quad , \quad i = 1, 2 \tag{5.8}$$

Expansion of (5.8) yields the two eigenvalues:

$$\left.\begin{array}{c} \gamma_f \\[2mm] \gamma_b \end{array}\right\} = \frac{1}{2} \left\{ x_{11} + x_{22} \pm [(x_{11} - x_{22})^2 + 4x_{12}x_{21}]^{1/2} \right\} \tag{5.9}$$

In particular, the following relation holds:

$$\gamma_f \gamma_b = x_{11}x_{22} - x_{12}x_{21} = | \underset{\sim}{x} | \tag{5.10}$$

Note that the upper and lower sign of (5.9) are allocated to γ_f and γ_b or, possibly in reversed order, to γ_b and γ_f. The choice is determined from the corresponding eigenvectors $\underset{\sim}{r}_f$ and $\underset{\sim}{r}_b$. These are given by:

$$\underset{\sim}{r}_f = \begin{bmatrix} x_{12} \\[3mm] \gamma_f - x_{11} \end{bmatrix} \tag{5.11}$$

$$\underset{\sim}{r}_b = \begin{bmatrix} x_{12} \\[3mm] \gamma_b - x_{11} \end{bmatrix} \tag{5.12}$$

The elements in the vectors γ_f and γ_b must satisfy certain sign requirements which determine the choice of sign in (5.9). The details are discussed at the end of this section.

The mathematical procedure is now to express the circuit rf variables, which are given by the vectors $\underline{b}_c(z_{n2})$ and $\underline{b}_c(z_{11})$ in (5.2), as superpositions of the two eigenvectors $\underline{r}_f$ and $\underline{r}_b$. Let

$$\underline{b}_c(z_{n2}) = C_f(z_{n2})\, \underline{r}_f + C_b(z_{n2})\, \underline{r}_b \tag{5.13}$$

$$\underline{b}_c(z_{11}) = C_f(z_{11})\, \underline{r}_f + C_b(z_{11})\, \underline{r}_b \tag{5.14}$$

Substituting these expansions into (5.2) and making use of (5.7), the resulting equation is in diagonal form:

$$\begin{bmatrix} C_f(z_{n2}) \\ \\ C_b(z_{n2}) \end{bmatrix} = \begin{bmatrix} \gamma_f & 0 \\ \\ 0 & \gamma_b \end{bmatrix} \begin{bmatrix} C_f(z_{11}) \\ \\ C_b(z_{11}) \end{bmatrix} \tag{5.15}$$

In component form:

$$C_f(z_{n2}) = \gamma_f C_f(z_{11}) \tag{5.16}$$

$$C_b(z_{n2}) = \gamma_b C_b(z_{11}) \tag{5.17}$$

What is the physical significance of the mathematical procedure of expansions into eigensolutions? It describes the resolution of the over-all rf circuit variables v_0 and i_0 into its forward and backward traveling components. These are described by their amplitudes C_f and C_b which, of course, are different at the input and output terminals.

Apparently, the gain of the forward and backward traveling waves are given by:

$$(\text{voltage gain})_f = \gamma_f \qquad (5.18)$$

$$(\text{voltage gain})_b = \frac{1}{\gamma_b} \qquad (5.19)$$

Hence, the respective gains are specified by the eigenvalue γ_f and the inverse eigenvalue $1/\gamma_b$. The two are related by (5.10) which can be expressed as:

$$(\text{voltage gain})_b = \frac{(\text{voltage gain})_f}{|\lambda|} \qquad (5.20)$$

This equation confirms the earlier condition (5.4) for backward wave oscillations, namely $|\lambda| = 0$. But (5.20) tells us more than (5.4). If the _forward_ gain, at the oscillation frequency, is zero, or very small, the procedure of putting $|\lambda| = 0$ is bound to be quite inaccurate, because the right-hand side of (5.20) is essentially a zero over zero expression.

The better, and correct, procedure is to determine the condition for infinite backward gain directly from (5.19), which is

$$\gamma_b = 0 , \qquad (5.21)$$

where γ_b is specified by the appropriate expression in (5.9). It follows immediately that this equation gives

$$\lambda_{11}\lambda_{22} - \lambda_{12}\lambda_{21} = |\lambda| = 0 \qquad (5.22)$$

44

Hence, it looks like (5.21) and (5.4) are entirely equivalent, but this is only from a superficial viewpoint. In any numerical iterative search routine, the end result is a small, but nevertheless finite value of γ_b or $|x|$. The search procedure depends on the <u>variations</u> of these functions <u>around</u> their zeros, which are quite different for γ_b and $|x|$ and favors the use of γ_b. The discussion in conjunction with (5.20) already emphasized this point. Moreover, the small, but finite value of γ_b obtained as the end result of the search procedure also tells us what the backward gain is under these circumstances, namely $1/\gamma_b$.

The forward and backward solutions are basically identified by the nature of the <u>eigenvectors</u>, rather than the eigenvalues. The latter can vary over a wide range because the forward and backward gain can be larger or smaller than unity, depending on the frequency and other operating parameters. Hence, under general conditions it is not easy to identify the forward and backward components from the two <u>eigenvalues</u>.

The forward wave is characterized by <u>positive power</u> flow which requires a positive real part of the impedance. In the eigenvector this requirement is reflected in the <u>signs</u> of the two vector elements. The real part of the elements must have the <u>same</u> sign.

Conversely, the eigenvector for the <u>backward</u> wave is characterized by <u>opposite</u> signs of the real parts of the vector elements.

The eigenvectors also provide us with direct information on the <u>characteristic impedances</u> for the forward and the backward waves. These questions are discussed in Section 5.4.1.

5.3 <u>PROPER PROCEDURE FOR DETERMINATION OF THE INHERENT BACKWARD WAVE INSTABILITY</u>

As noted, the procedure described in 5.1 is not entirely satisfactory. The proper procedure is based on the condition (5.21) rather than

45

(5.4). The real and imaginary parts are both zero. For convenience disregarding the subscript b we then have the two equations:

$$\gamma_r(I_0, \omega_r + j\omega_i) = 0 \tag{5.23}$$

$$\gamma_i(I_0, \omega_r + j\omega_i) = 0 \;, \tag{5.24}$$

which must be satisfied simultaneously. In order to provide a better understanding of backward wave oscillations, the frequency ω is assumed to be complex

$$\omega_c = \omega_r + j\omega_i \tag{5.25}$$

The two functional relationships (5.23) and (5.24) are sketched in Figure 5-2 as two sets of intersecting curves, with ω_i constant for each curve. The intersections between curves of the same complex frequency $\omega_r + j\omega_i$ represent the solution of the set (5.23) and (5.24), i.e., the condition for infinite backward wave gain. In the figure the solution is given by the dotted line B-C, which is naturally separated in two by the point A corresponding to a real frequency ω_s. Below A the solutions have positive imaginary frequency. Apparently this corresponds to an exponentially decaying solution in time, which therefore is stable. The solutions above the point A have negative imaginary frequency and grow exponentially with time. This is the unstable region. Hence, if we visualize that the current I_0 is increased from a low value, we are moving upward along the line B-C. The system is nice and stable until point A is reached. Point A represents the starting condition, which is characterized by a real oscillation frequency ω_s, and the starting current I_{0s}. If the current is increased upwards from A towards C, the system becomes unstable, with exponentially increasing rf amplitude. The amplitude is, of course, limited to a finite value through nonlinear effects.
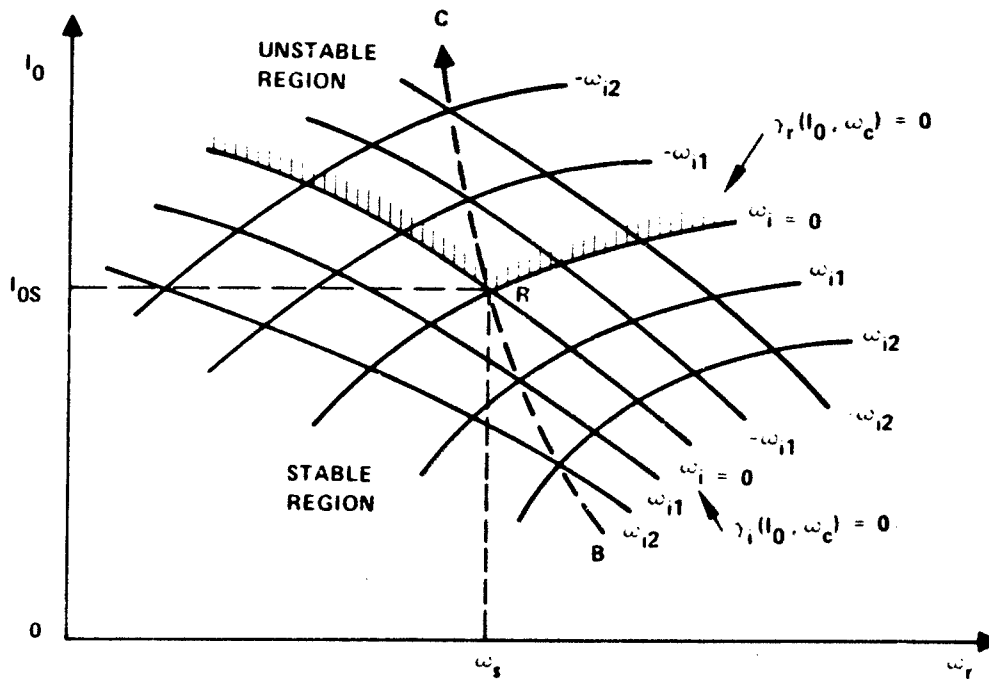
Figure 5-2   Sketch illustrating the nature of backward wave
instabilities.   The region above the shaded outline is
unstable.

47

5.4 THE EFFECT OF MISMATCHED INPUT AND OUTPUT TERMINALS ON BACKWARD WAVE INSTABILITIES

In the preceding treatment of the backward wave instability condition, it was assumed that the input and output terminals were matched. This can be considered to be the <u>basic</u> instability criterion. With no reflections at the input and output terminals, the instability is due entirely to the <u>inherent</u> feedback loops in the backward mode, and to the reflections taking place at the intersections between the uniform helix sections.

In this section we shall extend the analysis to the more general configuration of nonmatched input and output terminals. A schematic illustration of the configuration is shown in Figure 5-3.

In a practical situation one would like to determine the instability conditions for <u>each</u> of the two regions which are separated by the attenuato⁻. The actual configuration is shown schematically in Figure 5-4. The treatment is general enough to be applicable for this situation.

In the previously treated inherent instability condition, corresponding to matched input and output terminals, it was sufficient to consider equation (5.17) describing the backward wave gain. The equation (5.16) could be disregarded because of the forward wave amplitude C_f is zero under matched conditions. In the general case to be treated here, C_f is not zero. It will be convenient to introduce the <u>ratio</u> C_f/C_b at the input and output as new variables. But first, we must define the <u>characteristic impedances</u> of the forward and backward waves.

5.4.1 Forward and Backward Characteristic Impedances

The concept of characteristic impedance follows directly from (5.12)-(5.14). The impedance specifies the ratio of the normalized circuit voltage v_o
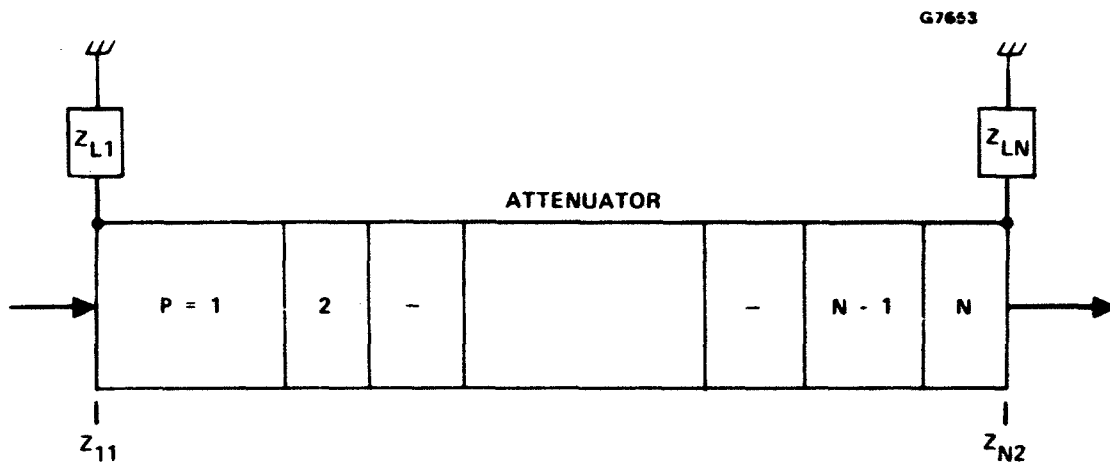
Figure 5-3   Schematic diagram wf a sectioned TWT with arbitrary
input and output loads Z_{L1} and Z_{LN}.
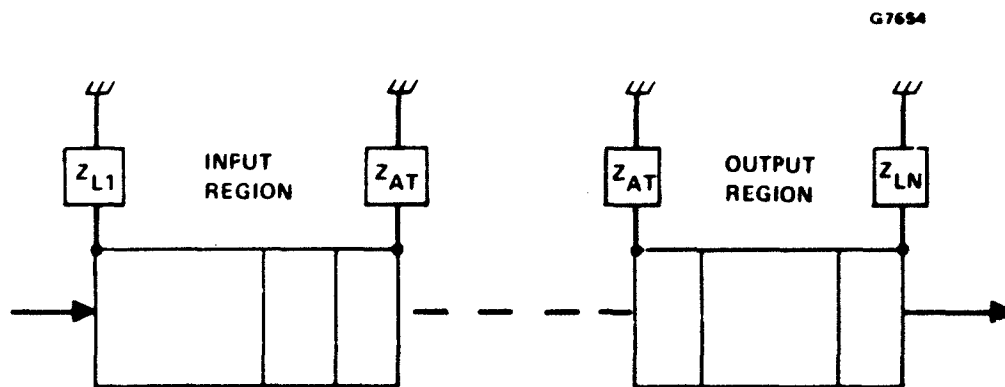
Figure 5-4   Sketch showing the TWT separated into two regions, with
the attenuator load Z_{At} serving as output load for the
first region and input load for the second region.

and the normalized circuit current i_0 for each of the two modes in the absence of the other. The normalized impedances follow in a straight-forward fashion from (5.11) and (5.12).

The _forward_ wave characteristic impedance $\mathcal{J}_f$ is given by:

$$\mathcal{J}_f = \left(\frac{v_0}{i_0}\right)_f = \frac{\lambda_{12}}{\gamma_f - \lambda_{11}} \tag{5.26}$$

Note that $\mathcal{J}_f$ is a _normalized_ impedance because v_0 and i_0 are normalized with respect to the dc voltage and current, respectively.

The _backward_ wave characteristic impedance $\mathcal{J}_b$ is given by

$$\mathcal{J}_b = \left(\frac{v_0}{i_0}\right)_b = \frac{\lambda_{12}}{\gamma_b - \lambda_{11}} \tag{5.27}$$

As already noted in Section 5.2, the real parts of $\mathcal{J}_f$ and $\mathcal{J}_b$ are positive and negative, respectively. But there is no reason to expect that $\mathcal{J}_b$ is equal to minus $\mathcal{J}_f$. Nor are these impedances specified directly by the cold circuit impedances. They reflect the properties of the over-all coupled beam and circuit system in the forward and backward directions, respectively.

5.4.2 The Reflections at the Input and Output Terminals

Introducing the ratio of the forward and backward mode amplitudes as a variable, we can use (5.16) and (5.17) to obtain the following relation:

$$\left(\frac{c_f}{c_b}\right)_n = \frac{\gamma_f}{\gamma_b}\left(\frac{c_f}{c_b}\right)_1 \quad , \tag{5.28}$$

50

where subscript n and 1 refer to the output and input terminals, respectively. We can easily determine the amplitude ratios from (5.13) and (5.14), together with a specification of input and output load impedances Z_{b1} and Z_{Ln}. At the output terminal

$$\left(\frac{v_o}{i_o} \right)_n = Z_{nL} \, G_o, \tag{5.29}$$

where

$$G_o = \frac{I_{DC}}{V_{DC}} \tag{5.30}$$

is the dc beam conductance.

At the input terminal we must reverse the sign because the rf circuit current is defined positive in the positive z-direction. Hence

$$\left(\frac{v_0}{i_0} \right)_1 = -Z_{1L} \, G_o \tag{5.31}$$

Using these two relations together with (5.13) and (5.14) we obtain:

$$\left(\frac{c_b}{c_f} \right)_n = \frac{1 - \dfrac{Z_{nL} \, G_0}{\mathcal{I}_F}}{\dfrac{Z_{nL} \, G_o}{\mathcal{I}_b} - 1} \tag{5.32}$$

$$\left(\frac{c_f}{c_b}\right)_1 = -\frac{1 + \dfrac{Z_{1L}\, G_o}{\mathcal{J}_b}}{1 + \dfrac{Z_{1L}\, G_o}{\mathcal{J}_f}} \qquad (5.33)$$

It is clear that the expressions (5.32) and (5.33) are the <u>reflection coefficients</u> at the output and input terminals, respectively. Denoting these by ρ_n and ρ_1, we have

$$\rho_n = \frac{1 - \dfrac{Z_{n L}\, G_o}{\mathcal{J}_f}}{\dfrac{Z_{n L}\, G_o}{\mathcal{J}_b} - 1} \qquad (5.34)$$

$$\rho_1 = -\frac{1 + \dfrac{Z_{1L}\, G_o}{\mathcal{J}_b}}{1 + \dfrac{Z_{1L}\, G_o}{\mathcal{J}_f}} \qquad (5.35)$$

One should note that the reflection coefficients are of a generalized nature compared to reciprocal transmission systems, because the characteristic impedances are different in the two directions.

The remaining step is to substitute (5.32) and (5.33) into (5.28). Also using the definitions of reflection coefficients, we obtain the following formula:

$$\gamma_b \rho_n \frac{1}{\gamma_b} \rho_1 = 1 \qquad (5.36)$$

This is the new instability condition which is characterized by unity <u>loop gain</u>. The condition of unity gain is clearer from inspections of

52

Figure 5-5, where the various factors in the product (5.36) are represented in the closed loop.

Equation (5.36) can be expressed in the equivalent way:

$$\gamma_b - \gamma_f \rho_1 \rho_n = 0 \qquad (5.37)$$

This equation represents the required generalization of (5.21). With matched terminals, ρ_1 and ρ_n are zero, and (5.37) reduces properly to (5.21).

If we define a <u>modified</u> γ_b' by the relation

$$\gamma_b' = \gamma_b - \gamma_f \rho_1 \rho_n \quad , \qquad (5.38)$$

it follows that the instability condition (5.37) is expressed by

$$\gamma_b' = 0 \qquad (5.39)$$

This implies that the general nonmatched configuration can be treated by exactly the same mathematical procedure as discussed in Section 5.3 for the <u>inherent</u> backward wave instability. We simply replace γ_b by γ_b', defined in (5.38), and proceed in exactly the same way.

With mismatched input and output terminals, i.e., with ρ_1 and ρ_n <u>both</u> different from zero, the required backward gain for the occurrence of instabilities is less than infinity. Hence, the starting current I_{0s} is expected to be reduced correspondingly.

This concludes the discussion of the formal structure of backward wave instabilities. We have established a general mathematical procedure by
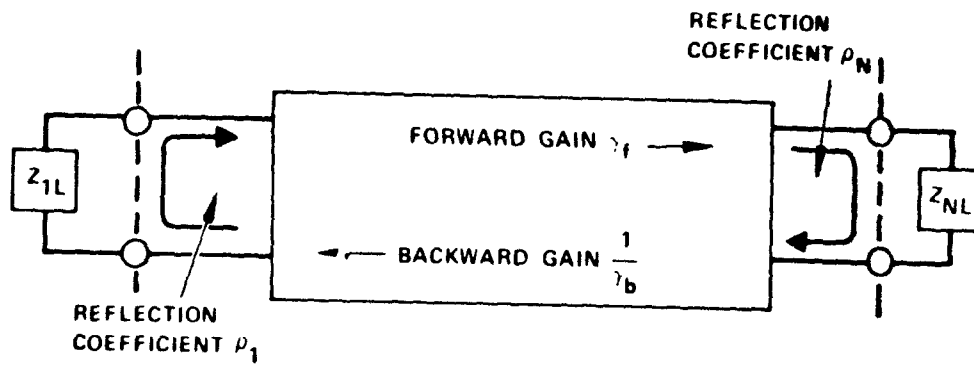
Figure 5-5   Schematic illustration of the condition (5.36) of unity
loop gain as criterion for backward wave oscillations.

which very general configurations of multisection TWTs can be analyzed
with regard to both forward and backward wave properties, in particular
backward wave instabilities. The important problems of _optimum_ _design_,
i.e., the design of multisection TWTs with the largest possible starting
current I_{0s} without undue sacrifice of forward wave characteristics, are
not approached analytically in the present work. The computer program
developed from the theory probably represents a better tool than any
approximate analytical methods, which conceivably could be developed from
the theory.

6.0 PLASMA REDUCTION FACTORS AND BEAM COUPLING
COEFFICIENTS FOR FORWARD AND BACKWARD MODES

The dispersion relation and state vectors for the coupled beam-circuit
system in a uniform helix section were given earlier by (4.5)-(4.7).
Among the parameters appearing in these relations are the plasma reduc-
tion factors $R_m^{(i)}$ and the coupling coefficients $f_m^{(i)}$, where $m = 0, \pm 1$
and $i = 1, 2, 3$.

A considerable amount of analytical work has been done in the course
of this program to determine these parameters under general focusing
conditions. The details are far too extensive to be included in the
final report. It is anticipated that a full account of beam wave
properties under general focusing conditions will eventually appear as
a separate technical report. In the present report we shall state a
few of the more significant results, in particular the plasma reduc-
tion factors and the beam-circuit coupling coefficients for confined flow.
We shall also discuss the more complex Brillouin focusing condition and
the corresponding backward wave characteristics.

6.1 BEAM MODEL

Plasma reduction factors and coupling coefficients are concepts that
depend on certain assumptions concerning the distribution of rf modu-
lations over the beam cross section. The details of the longitudinal
and transverse distributions depend in large measure on the _driving_
fields from the surrounding circuit. However, in order to represent
useful concepts in TWT design, the plasma reduction factors and coupling
coefficients should be largely independent of the details of the circuit,
except for a minimum of geometrical details such as radial dimensions
of the beam and the circuit.

This implies that one has to make reasonable assumptions concerning the distribution of beam modulations over the cross section. In the more traditional approaches it is common to use a Bessel function distribution, which is simply the basic term in an infinite normal mode expansion of space charge wave components. But this choice is dictated more from mathematical convenience rather than physical reality. In view of the fact that the edge regions of the beam are modulated more strongly than the central part, the Bessel function distribution is obviously not a good choice, because the $J_0(\beta_e r)$ Bessel function has its <u>maximum</u> at the center and decays towards the beam edge, i.e., the variation is exactly opposite from the actual situation.

With this in mind it seems logical to assume the very simplest distribution, which is that of <u>constant</u> velocity and displacement distributions over the beam cross section. Although this is not the actual physical distribution in the TWT, it is a better choice than the traditional Bessel function distribution.

Accordingly, the longitudinal and transverse dynamic variables for the $m = 0$ and the $m = \pm 1$ modes are specifed by the schematic diagrams in Figure 6-1. On this basis we have developed a complete field theory for determination of the associated fields which, in turn, specify the plasma reduction factors and coupling coefficients.

6.2 CONFINED FLOW

Confined flow represents a limiting case of focusing which is never quite achieved in a practical tube, because it requires infinite magnetic field, or zero beam current. But the condition can be approached to a degree which justifies the use of this concept.

As discussed earlier, confined flow is by far the simplest from a conceptual viewpoint. Since no beam rotation takes place, the $m = -1$ and

57

LONGITUDINAL MODULATION   TRANSVERSE MODULATION

a) m = 0

LONGITUDINAL MODULATION   TRANSVERSE MODULATION
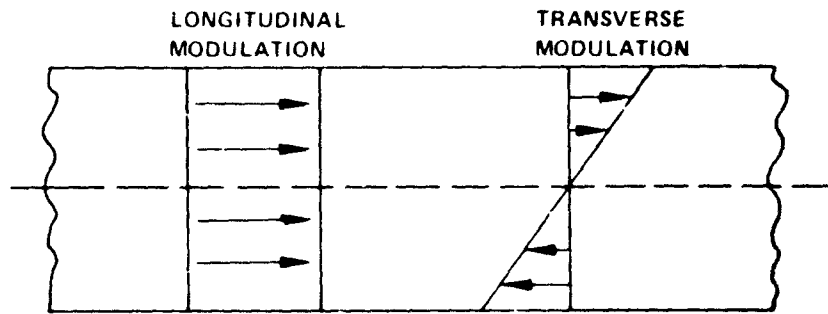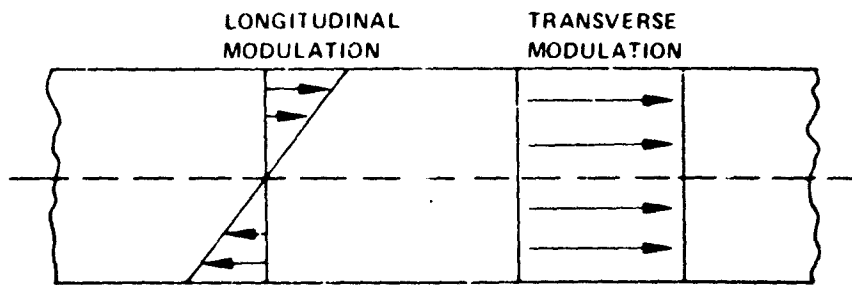
b) m = ·1

Figure 6-1   Schematic diagrams of the assumed distributions of the
dynamic variables over the beam cross section.
a) Fundamental mode, m = 0
b) Backward wave modes, m = ·1.

58

m = +1 beam modes are identical, except, of course, for the opposite angular variations. The plasma reduction factors and the coupling coefficients are the same for m = +1 and m = -1. But these differ from the corresponding factors of the fundamental mode m = 0.

6.2.1 Plasma Reduction Factors for Confined Flow

For the fundamental mode m = 0, the square of the plasma reduction factor is given by the expression:

$$R^2_{m=0} = 1 - 2 \frac{I_1(\gamma r_b)}{I_0(\gamma r_a)} G_{01}(\gamma r_a, \gamma r_b) \qquad (6.1)$$

The variables appearing in the equation are:

Beam radius, r_b

Helix radius, r_a $\qquad\qquad$ (6.2)

Propagation factor, γ

The functions $I_1(\gamma r_b)$ and $I_0(\gamma r_a)$ are modified Bessel functions, and $G_{01}(\gamma r_a, \gamma r_b)$ is defined as follows:

$$G_{01}(\gamma r_a, \gamma r_b) = I_0(\gamma r_a) K_1(\gamma r_b) + K_a(\gamma r_a) I_1(\gamma r_b) \qquad (6.3)$$

The propagation factor γ basically refers to the propagation factors $\beta^{(i)}$ of the three forward traveling modes, corresponding to i = 1, 2, and 3. But these are sufficiently close to justify the use of the same γ for all three components. Hence, for practical purposes

$$\gamma = \beta_e \qquad (6.4)$$

The plasma reduction factor for the $m = \pm 1$ waves is given by:

$$R^2_{m=\pm 1} = 1 + 2 \frac{(\gamma r_b)^2 K_2(\gamma r_b) - 2}{(\gamma r_b)^2}$$

$$- 2 \frac{I_2(\gamma r_b)}{I_1(\gamma r_a)} [G_{10}(\gamma r_a, \gamma r_b) - K_1(\gamma r_a)] \quad , \tag{6.5}$$

where

$$G_{10}(\gamma r_a, \gamma r_b) = I_1(\gamma r_a) K_0(\gamma r_b) + K_1(\gamma r_a) I_0(\gamma r_b) \tag{6.6}$$

The plasma reduction factors R_0 and $R_{\pm 1}$ are plotted in Figures 6-2 and 6-3 for several values of the beam-to-helix diameter ratio r_b/r_a.

From the expressions for R_0 and $R_{\pm 1}$ one can show that

$$\lim_{\gamma r_b \to 0} R_0 = \lim_{\gamma r_b \to 0} R_{\pm 1} = 0 \tag{6.7}$$

$$\lim_{\gamma r_b \to \infty} R_0 = \lim_{\gamma r_b \to \infty} R_{\pm 1} = 1 \tag{6.8}$$

The first of these two limiting cases, $R = 0$, corresponds to an infinitely thin beam in which case there are no longitudinal fields, only transverse field components. The second limiting case, $R = 1$, corresponds to infinite normalized beam radius, which essentially represents a one-dimensional case. The fields are pure longitudinal, and the transverse field components are zero.

PLASMA REDUCTION FACTOR R_0

0.8

0.7

0.6

0.5

0.4

0.3

0.2

0.1

0

0   0.25   0.5   0.75   1.0   1.25   1.5   1.75   2.0   2.25

0

0.67

0.80

$\dfrac{r_b}{r_a} = 1.00$

FUNDAMENTAL MODE, m = 0
CONFINED FLOW

$\beta_e r_b$
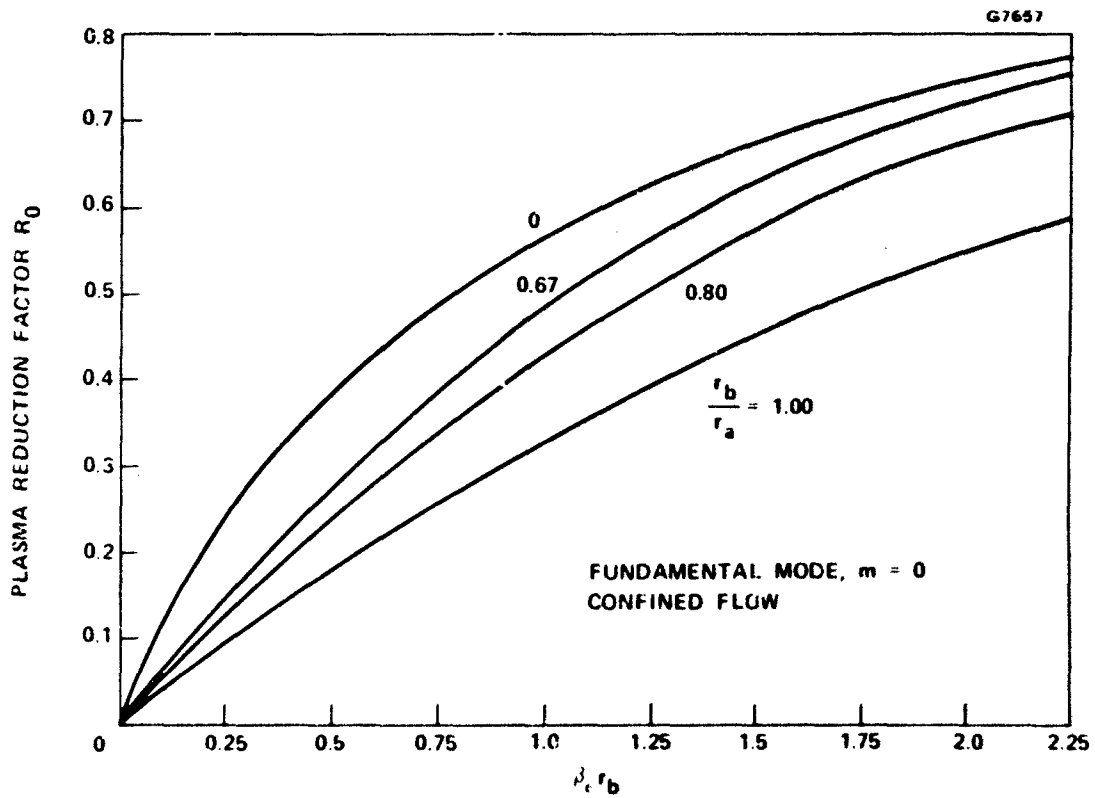
Figure 6-2   Plasma frequency reduction factor R_0 for forward wave
interaction and confined flow.
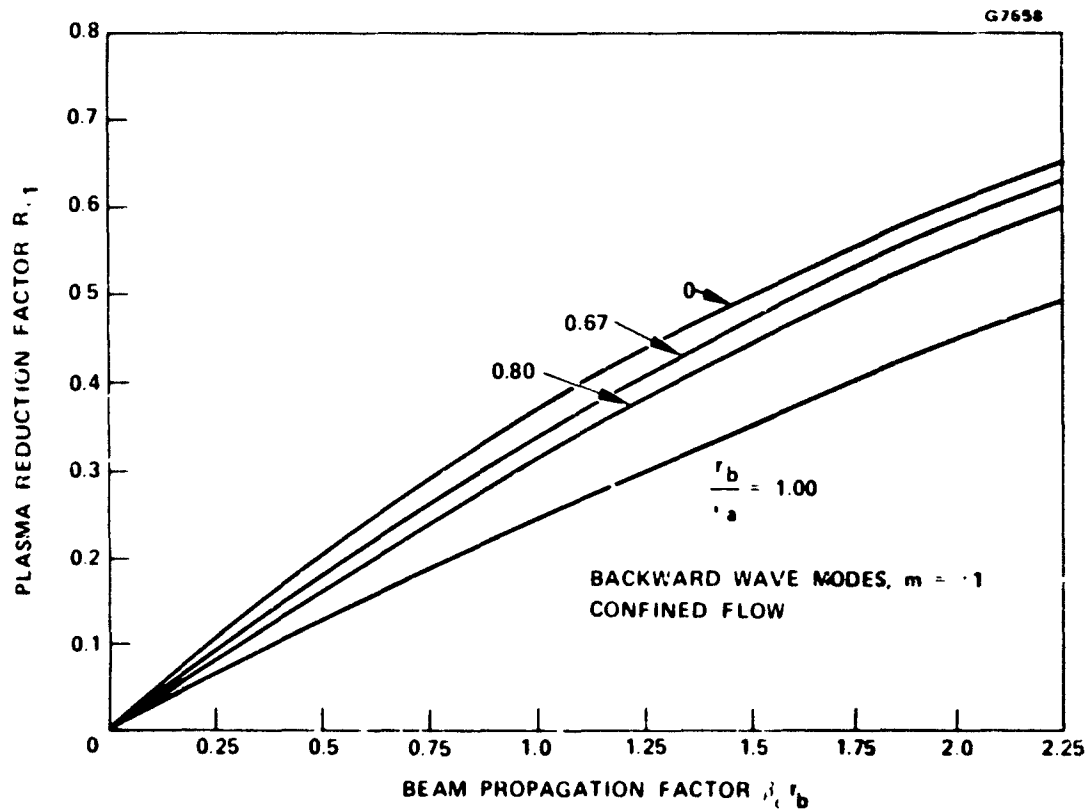
Figure 6-3   Plasma frequency reduction factor R_1 for backward wave interaction and confined flow.

6.2.2 Coupling Coefficients for Confined Flow

The coupling coefficient $f_m^{(i)}$ is a measure of the strength of the coupling between the beam and the current. The coefficient appears in the dispersion relation (4.5) and the state vectors (4.6).

For the fundamental mode, $m = 0$, the coupling coefficient is defined as the ratio of the circuit current I_c and the longitudinal current I_b in the beam

$$f_0 = \frac{I_c}{I_b} \qquad (6.9)$$

The coupling coefficient is obtained from the equation:

$$f_o = \frac{2I_1(\gamma r_b)}{\gamma r_b} \frac{1}{I_0(\gamma r_a)} \qquad (6.10)$$

The expression is plotted in Figure 6-4 for several values of the ratio r_b/r_a.

The mode symmetry in the backward traveling waves is such that the corresponding coupling coefficient does not have the same simple physical interpretation as (6.9) for the fundamental mode $m = 0$.

With reference to Figure 6-1b, the longitudinal current density in the $m = \pm1$ modes is specified by

$$i_b(r, \vartheta, z) = \hat{i}_b(z) \, e^{\pm j\vartheta} \, \beta_e r, \qquad (6.11)$$

where $\hat{i}_b(z)$ is interpreted as the one-dimensional equivalent of the constant current density in the fundamental mode. The actual current
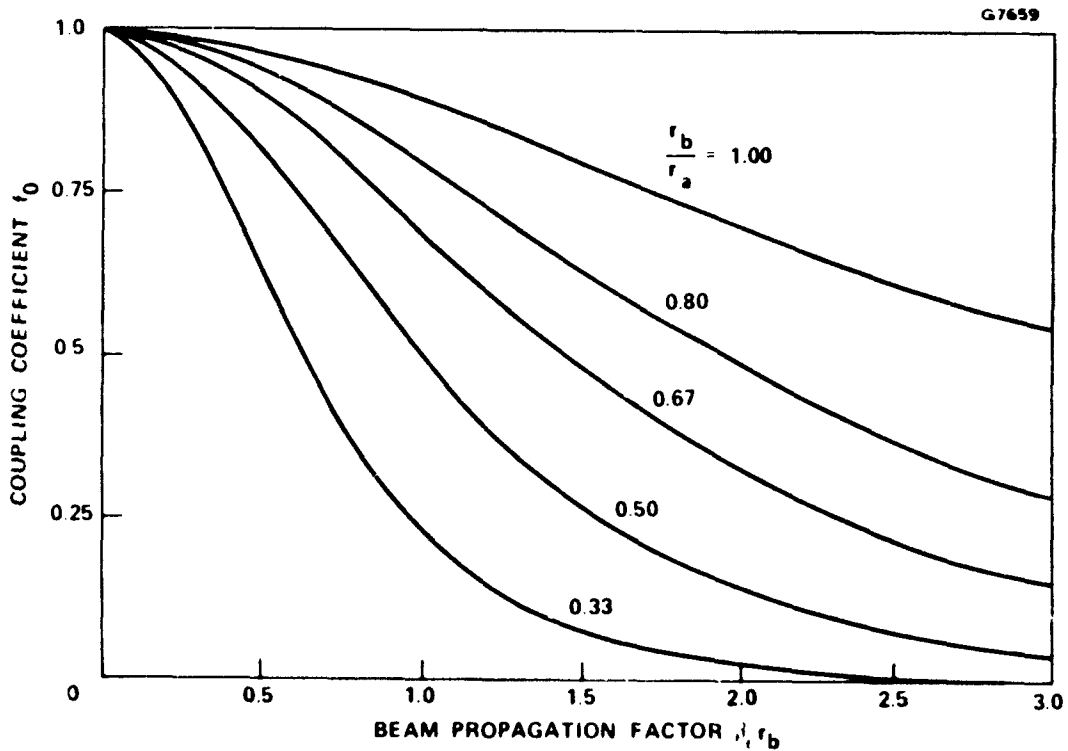
Figure 6-4   Beam-circuit coupling coefficient f_0 for forward wave interaction (m = 0) and confined flow.

density is proportional to the radius and varies azimuthally as exp $(\pm j\theta)$. The total integrated current is therefore zero. The entire theory in the present report is based on interpreting $\hat{i}_b(z)$ and (6.11) as an <u>equivalent one-dimensional current density</u>. The coupling coefficient $f_\pm$ is defined on the basis of this variable, in the following way:

$$f_{\pm 1} = \frac{\hat{i}_c(z)\ r_a d\theta}{\hat{i}_b(z)\ \frac{1}{2}\ r_b^2 d\theta} \qquad (6.12)$$

where $\hat{i}_c(z)$ is the <u>surface</u> current density in the surrounding circuit, in the m = ±1 mode.

Evaluation of the coupling coefficient $f_{\pm 1}$ yields the following expression:

$$f_{\pm 1} = \frac{2}{I_1(\beta_e r_a)} \left[I_0(\beta_e r_b) - \frac{2I_1(\beta_e r_b)}{\beta_e r_b} \right] \qquad (6.13)$$

The equation is plotted in Figure 6-5. It is noted that $f_{\pm 1}$ can be larger than unity. This is simply due to the fact that the coupling coefficient for the antisymmetric backward wave modes does not have the same simple physical interpretation as the corresponding coefficient f_0 for the fundamental mode. In particular, the numerical value of $f_{\pm 1}$ depends on how we define the "one-dimensional equivalent beam current density" $\hat{i}_b(z)$. The definitions used in the present work are stated in (6.11) and (6.12), and all remaining equations are consistent with these definitions.

6.3 BRILLOUIN FLOW

In the present program an extensive analysis has been made of the nature of electron beam waves in a general, balanced beam model. This
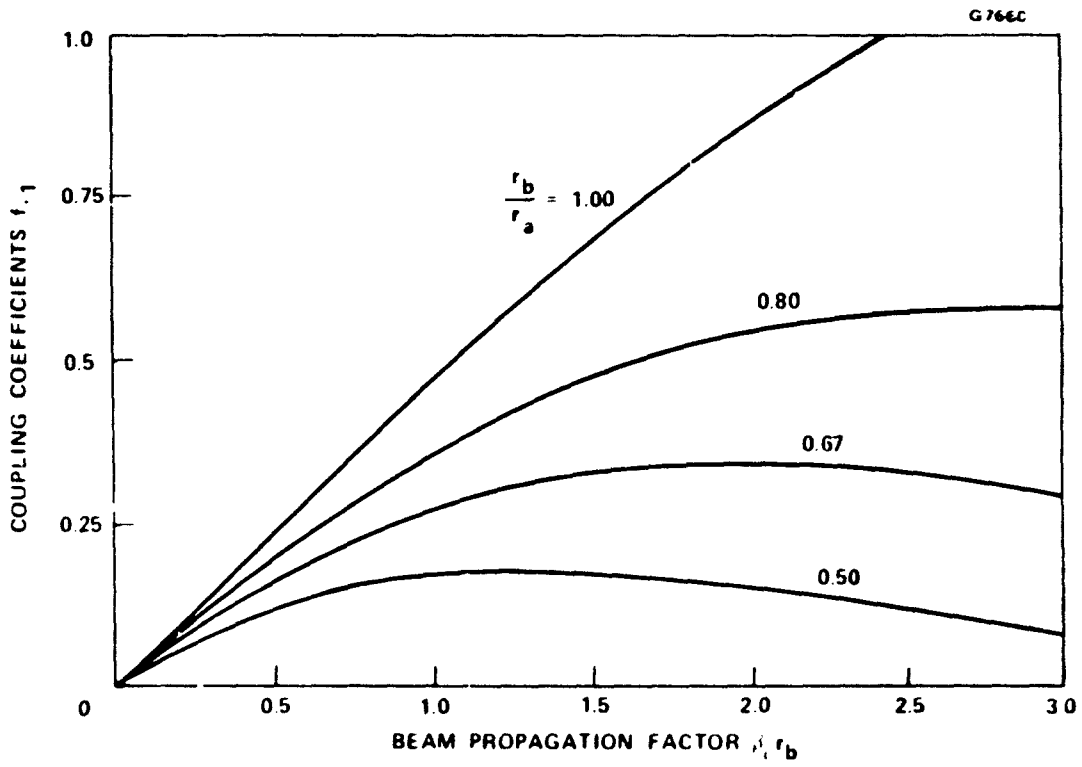
Figure 6-5   Beam-circuit coupling coefficient f_{+1} for backward wave interaction ($m = \pm 1$) and confined flow.

model includes, as special cases, the confined flow condition treated in the previous section and the Brillouin flow condition. The dispersion relation, and thereby the plasma reduction factors and the coupling coefficients, are specified by an _implicit_ equation of sixth order. For the simple case of confined flow one can evaluate these factors explicitly. However, for Brillouin beams the situation is not so simple. The roots of the sixth order equation must be solved by numerical computer procedures, and only fairly crude approximations can be obtained analytically.

The roots of the sixth order equations determine a set of _six_ beam waves. In addition to the regular space charge waves the beam supports two _cyclotron_ waves and two quasisynchronous displacement waves.

The analysis has been carried all the way to a detailed specification of all the elements in the sixth order dispersion relation. But the establishment of numerical solutions and interpretations of the characteristics of the beam waves would represent a large effort much beyond the scope of the present program. Therefore, the following treatment is limited to presenting approximate solutions for the backward wave characteristics in Brillouin beams.

6.3.1 Plasma Reduction Factors for the Backward Waves (m = ±1) in Brillouin Flow

For confined flow we found that the plasma reduction factors for the m = +1 and m = -1 modes were the same. The reason for this result is that the beam motion is purely longitudinal. Hence, for reasons of symmetry there can be no difference in the behavior of the m = +1 and m = -1 modes, except, of course, the opposite azimuthal variations.

On the other hand, for nonconfined flow, such as the Brillouin condition, the m = +1 and m = -1 modes have different plasma reduction

factors. They also depend on the <u>direction</u> of the dc magnetic
focusing field.

An approximate perturbation procedure is reasonably accurate for the
m = ±1 modes because this particular symmetry maintains the beam cross
section everywhere under rf conditions. Hence, the transverse dis-
placement is not likely to play an important role for the space charge
field. On the other hand, for Brillouin flow, the circularly sym-
metric mode, m = 0, is characterized by uniform radial expansions and
contractions, which clearly contribute to the axial space charge field
and therefore to the plasma reduction factor. Accordingly, we limit
the approximate procedure to the m = ±1 backward modes.

The results for the m = +1 mode can be stated as follows:

Slow wave: $$R_{+1,s} = R_{\pm 1} + \frac{1}{\sqrt{2}}$$ (6.14)

Fast wave: $$R_{+1,b} = R_{\pm 1} \pm \frac{1}{\sqrt{2}}$$ (6.15)

where $R_{\pm 1}$ is the plasma reduction factor for <u>confined</u> flow, specified
by (6.5) or Figure 6-3. The upper signs in (6.14) and (6.15) apply for
<u>positive</u> direction of the dc magnetic focusing field, the lower sign
for <u>negative</u> direction of the field.

For the m = -1 mode the corresponding equations are:

Slow wave: $$R_{-1,s} = R_{\pm 1} \pm \frac{1}{\sqrt{2}}$$ (6.16)

Fast wave: $$R_{-1,b} = R_{\pm 1} + \frac{1}{\sqrt{2}} ,$$ (6.17)

where the upper and lower signs refer to the same conditions of
focusing as stated above.

According to these relations the plasma reduction factors depend on the
sign of m, and the sign of the dc magnetic field. The following general
relations apply:

$$R_s(m, B_0) = R_s(-m, -B_0) \qquad (6.18)$$

$$R_f(m, B_o) = R_f(-m, -B_0) \qquad (6.19)$$

The consequences of these relations for backward wave oscillations under
Brillouin flow conditions are such that we expect the starting condition
to be different for reversed direction of magnetic field. Or equiva-
lently, as shown by the general relations (6.14)-(6.19), a right-handed
and a left-handed helix do not have the same starting conditions for
the same direction of magnetic field. This difference is expected to
affect both the starting current and the frequency of oscillation,
and should be observable experimentally in uniform Brillouin focused
TWTs.

In a periodically focused TWT, the focusing fields in alternate sections
correspond to the positive and negative Brillouin field. Accordingly,
the plasma reduction factors alternate between the upper and lower values
in (6.14)-(6.17). The synchronization condition for backward wave
oscillations also changes periodically with the same periodicity. Due
to the dominant use of periodic Brillouin focusing in TWTs, an impor-
tant question is how to approach the problems associated with the
periodic nature of the electron beam. We could suggest to incorporate
the periodic sections into the over-all forward and backward inter-
action system analyzed in Chapters 4 and 5. In principal, one could
think of introducing the concept of a "sectioned beam" in the same way

as done for sectioned helices. However, this is more difficult for the beam, because of mode conversions taking place at the field reversals, but it may still be possible to implement. It would require more detailed knowledge of all the six beam modes discussed earlier, and of the appropriate matching conditions of the field reversals. In itself this is a considerable task far beyond the scope of the present program.

In lack of such a description we are forced to accept approximate procedures. If we insist on using one single plasma reduction factor for the entire length of the periodically Brillouin focused beam, the best choice appears to be the average value of the reduction factors in alternate sections. But from (6.14)-(6.17) we observe that the average values are just $R_{\pm 1}$, i.e., the reduction factor for confined flow. Hence:

$$(\overline{R_{\pm 1}})_{Brill} = (R_{\pm 1})_{confined} \tag{6.18}$$

In this approximate description the periodic Brillouin beam looks like a confined beam, as far as the $m = \pm 1$ modes are concerned. Physically, this picture is quite acceptable in view of the fact that the average dc rotational frequency is zero, i.e., the same as in confined flow. In the same approximation, we would expect the average coupling coefficient to be equal to the coupling coefficient for confined flow:

$$(\overline{f_{\pm 1}})_{Brill} = (f_{\pm 1})_{confined} \tag{6.19}$$

This concludes the discussion of backward wave characteristics for the Brillouin focused beam. Further analysis is required of the special problems of periodic Brillouin focusing and its implementation in the over-all forward and backward wave system described in Chapters 4 and 5.

70

LIST OF SYMBOLS

$\underset{\sim}{a}$	Column vector specifying the rf variables along the tube.
$\underset{\sim}{a}_b$	Column vector for the backward wave mode.
$\underset{\sim}{a}_f$	Column vector for the forward wave mode.
$\underset{\sim}{a}_m$	Column vector for the mth space harmonic component.
$\underset{\sim}{b}$	Overall column for the rf variables.
$\underset{\sim}{b}_c$	Circuit part of $\underset{\sim}{b}$.
$\underset{\sim}{b}_e$	Beam part of $\underset{\sim}{b}$.
c	Velocity of light in vacuum.
d	Pitch of helix.
e	Charge of the electron.
$f_m^{(i)}$	Coupling coefficient of the ith mode of the mth space harmonic.
i_b	Backward wave mode circuit current normalized to the dc current (mode m = 0).
$i_{b,m}$	Backward wave mode circuit current normalized to the dc current (mode m).
$i_{f,m}$	Forward wave mode circuit current normalized to the dc current (mode m).
m	Space harmonic number.
m_o	Rest mass of electron.
m_ℓ	Relativistic mass of electron in the longitudinal direction.
m_t	Relativistic mass of electron in the transverse direction.
$\underset{\sim}{q}_m^{(i)}$	The ith component of the state vector for the mth space harmonic.

r_a Helix radius.

r_b Beam radius.

$\underset{\sim}{r}_f$ Eigenvector of the $\underset{\sim}{\chi}$-matrix.

$\underset{\sim}{r}_b$ Eigenvector of the $\underset{\sim}{\chi}$-matrix.

s RF displacement.

t_o Time.

v_o DC beam velocity.

v_b Backward wave mode circuit voltage normalized to the dc voltage (mode $m = 0$).

$v_{b,m}$ Backward wave mode circuit voltage normalized to the dc voltage (mode m).

$v_{f,m}$ Forward wave mode circuit voltage normalized to the dc voltage (mode m).

$v_{c,m}$ Phase velocity of the mth space harmonic component of the circuit alone.

$\mathscr{Y}_f$ Forward wave mode overall characteristic impedance of the TWT.

$\mathscr{Y}_b$ Backward wave mode overall characteristic impedance of the TWT.

$\underset{\sim}{A}_m$ Normal mode vector of the mth space harmonic.

$B_m^{(i)}$ Normalized propagation factor of the ith mode of the mth space harmonic.

C_f Normal circuit mode amplitude of forward mode in the TWT.

C_b Normal circuit mode amplitude of backward mode in the TWT.

$\underset{\sim}{D}_m$ Diagonal matrix containing the normalized propagation factors $B_m^{(i)}$.

$\vec{E}_m(\vec{r})$	Electric field of the mth space harmonic component.
$G_{01}(\beta r_a, \beta r_b)$	Combination Bessel function.
I_o	DC beam current.
$\underset{\sim}{I}$	Inverse of transmission matrix T.
$I_o(\beta_{er})$	Modified Bessel function of first kind and zero order.
$I_1(\beta_{er})$	Modified Bessel function of first kind and first order.
$K_o(\beta_{er})$	Modified Bessel function of second kind and zero order.
$K_1(\beta_{er})$	Modified Bessel function of second kind and first order.
L	Normalized length of one helix section.
$\underset{\sim}{M}_e$	Overall state matrix for left-handed helix.
$\underset{\sim}{M}_r$	Overall state matrix for right-handed helix.
$\underset{\sim}{P}_m$	Submatrix of state matrix $\underset{\sim}{Q}'_m$.
$\underset{\sim}{Q}'_m$	State matrix of the mth space harmonic component.
$\underset{\sim}{Q}_m$	Part of $\underset{\sim}{Q}'_m$.
$R_m^{(i)}$	Plasma reduction factor of the ith mode of the mth space harmonic component.
S_m	Normalized displacement of the mth space harmonic component.
$\underset{\sim}{T}$	Overall transmission matrix.
$\underset{\sim}{T}(P)$	Transmission matrix of section p.

T_{11})

T_{12} (

T_{21} (Submatrices in the overall transmission matrix T.

T_{22})

U_m Normalized rf beam velocity of the mth space harmonic component.

V_o DC beam velocity.

W_m Submatrix of Q'_m.

z_o Normalized length.

z_{cm} Circuit impedance of the mth space harmonic, referred to the circuit location $r = r_a$.

z_{n2} Normalized position at output end of last section.

z_{11} Normalized position at input end of first section.

Z_{12} Load impedance at the input.

Z_{nL} Load impedance at the output.

β_m Propagation factor of the mth space harmonic.

γ Relativistic factor.

γ_f Eigenvalue of the χ-matrix.

γ_b Eigenvalue of the χ-matrix.

ϵ_o Permittivity of free space.

κ_m Loss parameter of the mth space harmonic component.

Γ_1 Reflection coefficient at the input end of the TWT.

Γ_m Reflection coefficient at the the output end of the TWT.

LIST OF SYMBOLS (CONTINUED)

ω	Angular frequency.
ω_c	Complex angular frequency.
ω_i	Imaginary angular frequency.
ω_{po}	Non-relativistic plasma frequency.
ω_p	Relativistic plasma frequency.
$\hat{\Omega}_p$	Plasma frequency normalized to the operating frequency.
$\underset{\sim}{\chi}$	A 2 x 2 submatrix equal to $\underset{\sim}{T}_{11}$.
$\left.\begin{array}{l}\chi_{11}\\\chi_{12}\\\chi_{21}\\\chi_{22}\end{array}\right\}$	The elements of $\underset{\sim}{\chi}$.
$\lvert\chi\rvert$	Determinant of $\underset{\sim}{\chi}$.
$\lvert\chi\rvert_r$	Real part of $\lvert\chi\rvert$.
$\lvert\chi\rvert_i$	Imaginary part of $\lvert\chi\rvert$.

MISSION
of
Rome Air Development Center

RADC plans and executes research, development, test and selected acquisition programs in support of Command, Control Communications and Intelligence (C^3I) activities. Technical and engineering support within areas of technical competence is provided to ESD Program Offices (POs) and other ESD elements. The principal technical mission areas are communications, electromagnetic guidance and control, surveillance of ground and aerospace objects, intelligence data collection and handling, information system technology, ionospheric propagation, solid state sciences, microwave physics and electronic reliability, maintainability and compatibility.